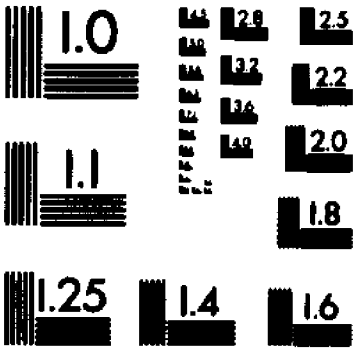

MICROCOPY RESOLUTION TEST CHART
NATIONAL BUREAU OF STANDARDS
STANDARD REFERENCE MATERIAL 1010a
(ANSI and ISO TEST CHART No. 2)

Goonatillake, Haupage Wimalasiri

MODIFICATIONS OF PORPHYRINS UPON ADSORPTION ONTO POROUS VYCOR GLASS

City University of New York PH.D. 1986

PLEASE NOTE:

In all cases this material has been filmed in the best possible way from the available copy. Problems encountered with this document have been identified here with a check mark __✓__.

1. Glossy photographs or pages _____
2. Colored illustrations, paper or print _____
3. Photographs with dark background _____
4. Illustrations are poor copy _____
5. Pages with black marks, not original copy _____
6. Print shows through as there is text on both sides of page _____
7. Indistinct, broken or small print on several pages __✓__
8. Print exceeds margin requirements _____
9. Tightly bound copy with print lost in spine _____
10. Computer printout pages with indistinct print _____
11. Page(s) _____ lacking when material received, and not available from school or author.
12. Page(s) _____ seem to be missing in numbering only as text follows.
13. Two pages numbered _____. Text follows.
14. Curling and wrinkled pages _____
15. Dissertation contains pages with print at a slant, filmed as received __✓__
16. Other _____

_____

_____

University
Microfilms
International

MODIFICATIONS OF PORPHYRINS UPON ADSORPTION ONTO POROUS VYCOR GLASS

by

HAUPAGE W.GOONATILLAKE

A dissertation submitted to the Graduate Faculty in Chemistry in partial fulfillment of the requirements for the degree of Doctor of Philosophy, The City University of New York

1986

This manuscript has been read and accepted for the Graduate Faculty in Engineering in satisfaction of the dissertation requirement for the degree of Doctor of Philosophy.

1/3/86
date

Thomas C. Stellar, Harry D. Saltzberg
Chairman of Examining Committee

1/7/86
date

Executive Officer

Supervisory Committee

The City University of New York

Abstract

MODIFICATION OF PORPHYRINS UPON ADSORPTION ONTO POROUS VYCOR GLASS

by

Haupage W. Goonatillake

Advisors: Professors Thomas C. Strekas and Harry D. Gafney

Corning's code 7930 porous Vycor glass (PVG) pretreated at 550°C in air is used as the solid support for adsorption of tetraphenylporphyrin (TPP) and metallotetraphenylporphyrin complexes from methylene chloride solutions. Immediate color changes and absorption spectral changes of the adsorbate are observed, which suggest chemical modifications. These modifications are characterized via absorption, emission, resonance Raman and electron spin resonance spectroscopies. The acidity of the PVG surface (measured pH value between 3 and 4) plays a role in the protonation phenomena of the adsorbates. The formation of the π-cation radicals on the surface of PVG, the one electron oxidation product of the porphyrin ring, is identified using esr spectroscopy in the absence of air. A hyperfine structure similar to the reported hyperfine pattern of π-cation radicals of porphyrins in solution is observed. In the presence of air the cation radical is

further oxidized to the dication which then reacts with nucleophilic surface silanol groups to form the isoporphyrins, the porphyrin derivatives in which the nucleophile is attached to one of the meso positions of the ring. The formation of the isoporphyrin is evidenced by absorption bands at 770 nm and 840 nm and resonance Raman bands. Presence of oxygen is found to be necessary for the formation of the isoporphyrin. Possible mechanisms for the generation of π-cation radicals via interaction with Lewis and Bronsted acid sites on the surface of PVG are discussed.

ACKNOWLEDGEMENT

I am indebted to my thesis advisors Professors Thomas Strekas and Harry Gafney for their guidance and advice during the course of this thesis research. I am especially grateful to Professor Strekas for many ways that he helped me both as a teacher and as a friend during my years here. His ideas and instruction made much of this thesis possible.

The many suggestions of Professor David Baker have been especially valuable. My thanks go to all my colleagues as well as to the faculty and staff of the chemistry department at Queens College for being very helpful. I wish to acknowledge with thanks the help from Professor David Locke when I joined the graduate school.

To my wife Shanthi and daughter Samantha, I thank for their encouragement, understanding and unfailing patience. And most of all, I remember my parents with gratitude, for everything that they have done for me.

TABLE OF CONTENTS

LIST OF TABLES

LIST OF FIGURES

1. INTRODUCTION

A GENERAL INTRODUCTION

In nature many important central biochemical functions are performed by porphyrins. For example all life on earth relies directly on the central role of chlorophylls and cytochromes in photosynthesis by means of which energy from sunlight is converted to chemical energy. In mammals, oxygen is transported by hemoglobin and stored by myoglobin. During respiration , oxygen is reduced to water by transfer of four electrons from cytochrome oxidase via a series of cytochromes.

During the first half of this century, massive contributions to our knowledge of chemistry of porphyrins and metalloporphyrins and related compounds were accumulated. A major publication in the field appeared in 1964[1], in which all the available data at that time were documented. This book, focused on the avenues for research open in this field. In 1973, at a symposium held at the New York academy of sciences[2], information available at the time was reviewed by prominent scientists in the field.

Falk's monograph was later revised and expanded[3]. More recently, seven volumes containing review articles on all aspects of chemistry of porphyrins were edited by D.Dolphin[4].

B. ELECTRONIC STUCTURE OF PORPHYRINS AND METALLOPORPHYRINS.

The basic porphyrin macrocycle is shown below (1).

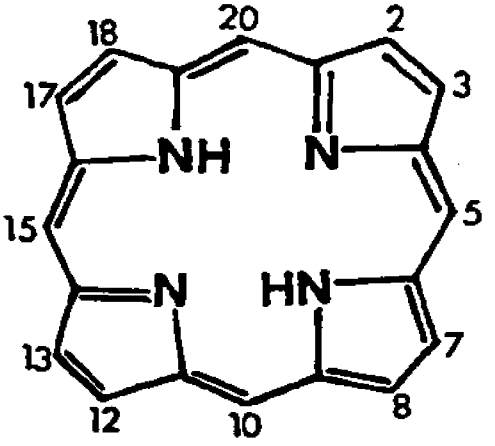

(1)

Porphyrin derivatives are commonly formed by substitution for H atoms on pyrrole rings (positions 2,3,7,8,12,13,17,18) or H atoms at meso positions (5,10,15,20). Octaethyl porphyrin (OEP) (ethyl groups at pyrrole positions) has been frequently used (ref 5) because the peripheral substitution pattern resembles that of the native porphyrins while preserving a high degree of symmetry. However, it is not easily prepared and is rather expensive. Therefore the more easily obtained 5,10,15,20-tetraphenylporphyrin (TPP) has been more widely used.

The porphyrin macrocycle is highly conjugated, and a number of resonance forms can be written. There are 22 electrons, but only 18 of these can be included in any one delocalization pathway. This conforms with Huckel's 4n+2 rule for aromaticity.

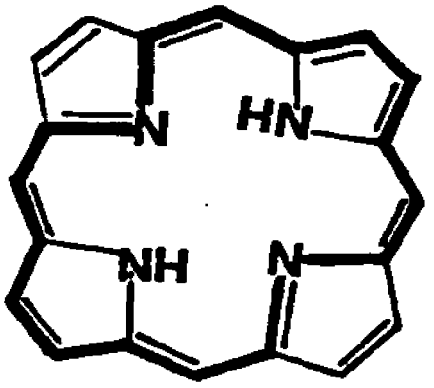

(2)

In the free base (2), because the proton positions are fixed there is only a single path of conjugation of the 18 π electrons on an 18-atom ring. The nitrogen atoms of the free base that lie on the path of conjugation have lone pair electrons within the plane that do not enter the π system.

Each atom on the conjugation path contributes one p electron which makes it an 18 atom, 18 π electron system.

When a metalloporphyrin is formed two H atoms from the ring are lost with the formation of the dianion which then complexes with the metal ion (3, 4 and 5).

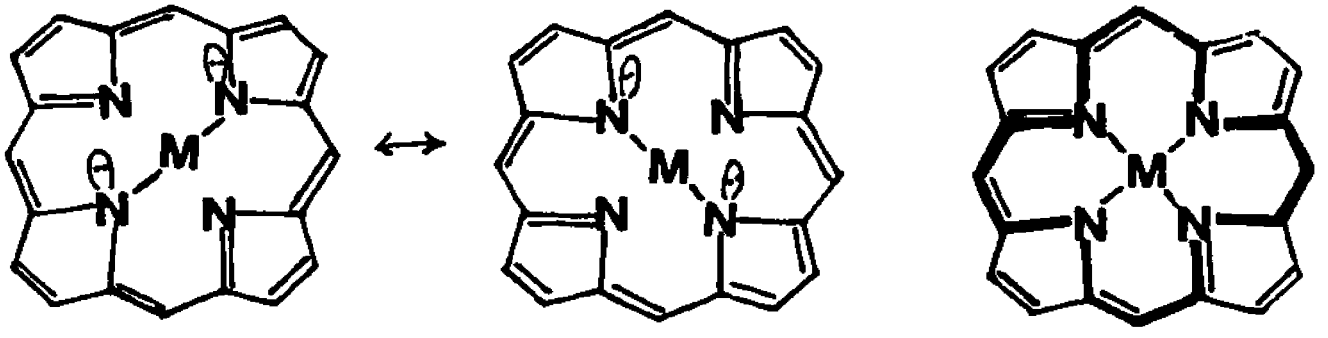

(3) (4) (5)

In this case the "imino" nitrogens are included in the path of conjugation which means there are 18 electrons, one from each member of the conjugated ring and two each from two N atoms. This makes it a 16 membered 18 π electron system. The other parent macrocycles are chlorin (6), Phorbin (7), Bacteriochlorin (8) and porphyrinogen (9).

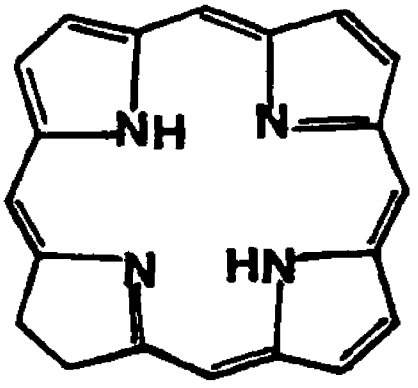

(6)

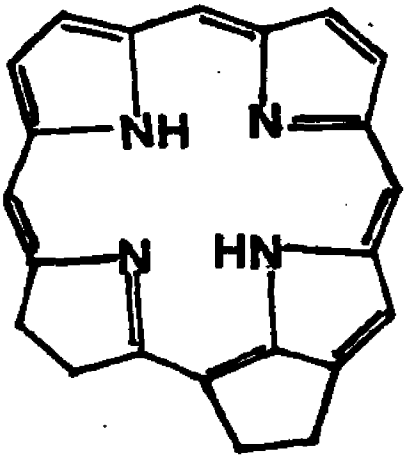

(7)

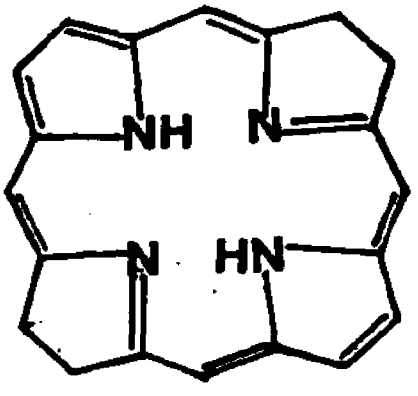

(8)

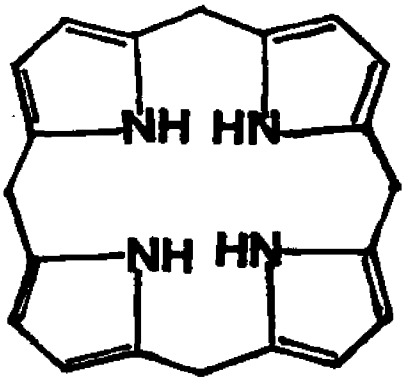

(9)

C. PROPERTIES OF PORPHYRINS AND METALLOPORPHYRINS

(a) Absorption Spectra

The absorption spectra of all metalloporphyrins consist of an exceedingly intense ($\epsilon \sim 10^5$ M^{-1} cm^{-1}) Soret band (or B band) between 380 and 420 nm and a pair of weaker ($\epsilon \sim 10^4$ M^{-1} cm^{-1}) bands called α and β (or Q_{0-0} and Q_{1-0}) bands. These features are illustrated in Fig. 1 for zinc tetrapenylporphyrin (ZnTPP). In addition, there can be weaker bands in the visible region that are due to charge transfer transitions from the porphyrin to the metal. In some cases, mixing between α, β or Soret and porphyrin-metal charge transfer can occur , resulting in rather complex absorption spectra.

Using the D_{4h} point group for the metalloporphyrin molecule, molecular orbital studies[6] predict that the highest filled orbitals are of a_{1u} and a_{2u} symmetry and that the lowest empty orbital is of e_g symmetry. The band is due to the $a_{2u}(\pi)$ ------- $e_g(\pi^*)$ electronic transition and the Soret band to the $a_{1u}(\pi)$ -----$e_g(\pi^*)$ transition[7]. Both transitions are of E_u symmetry, polarized in the plane of the molecule and are allowed. Configuration interaction between these nearly degenerate transitions leads to addition and cancellation of the transition dipoles resulting in the intense Soret and weaker α bands, respectively.

Figure 1 : Absorption spectrum of ZnTPP in methylene chloride solution to show the characteristic features of the absorption spectra of porphyrins. The Soret band (B_{0-0}) at 419 nm is about 10 times more intense than the α band (Q_{0-0}) at 585 nm and the β band (Q_{1-0}) at 545 nm.

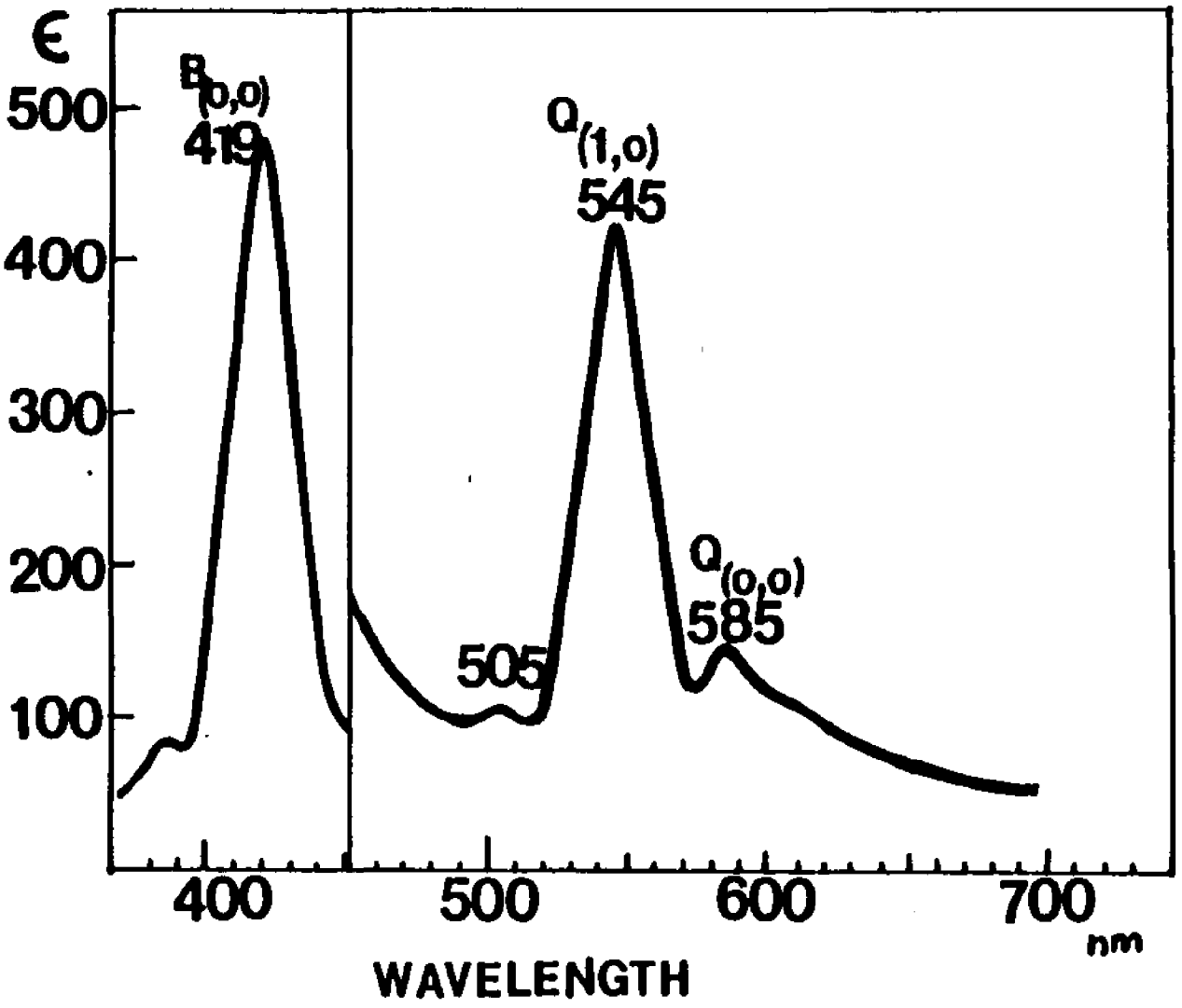
ε
500
400
300
200
100
B(0,0)
419
Q(1,0)
545
Q(0,0)
585
505
400
500
600
700
nm
WAVELENGTH

The β band is a vibronic side band of the α band. i.e.while the α band is due to a pure electronic transition (with no change in vibrational quantum number) the β band includes one mode of vibrational excitation and is denoted Q_{1-0}. In going from metalloporphyrins (16 membered conjugated ring) to free base porphyrin (18 membered ring) the symmetry of the molecule changes from D_{4h} to D_{2h}. Thus, $Q_{(0-0)}$ splits into $Q_{x(0-0)}$ and $Q_{y(0-0)}$ separated by about 3000 cm^{-1} for free base porphyrin. Each band has a vibronic overtone, $Q_{x(1-0)}$ and $Q_{y(1-0)}$ respectively. Therefore, the absorption spectrum of free base consists of four bands in the visible region.

Metalloporphyrins have been classified into two broad classes, namely "regular" and "irregular", depending on absorption and emission properties[7]. The regular metals contain only closed shells while the irregular metals contain partly filled shells. The same metal can be regular or irregular depending on the oxidation state. In regular metalloporphyrins the metal has only a small effect on the ring, and absorption and emission spectra can be explained in terms of porphyrin π - π^* transitions. In the case of irregular porphyrins metal orbitals have a stronger effect on absorption and emission, either through stronger mixing with the ring orbitals or through the introduction of new low energy optical transitions.

(b) Luminescence of porphyrins and metalloporphyrins.

Most free base porpnyrins show strong fluorescence at room temperature. This provides a very sensitive method for their detection and determination. The first systematic study of the influence of different metals on porphyrin fluorescence and phosphoresence was reported by Becker and Kasha in 1955[8]. Tables 1 and 2 summarize the emission properties of free base and metalloporphyrins at room temperature in fluid medium and at liquid nitrogen temperature (77 K)[9]. The closed shell metals having empty or full d shells form complexes with octa-alkyl and TPP that generally show only fluorescence at room temperature and both fluoresence and phosphorescence at 77 K. Earlier studies indicated only phosphorescence for porphyrin complexes with diamagnetic transition metal ions having partially filled d shells (Mn, Fe, Co, and Ni)[10]. Subsequent studies have indicated that complexes of Ni and Co do not emit[11] Strong phosphorecence is observed in Pd and Pt (d^8) complexes at R.T. and 77 K. The small singlet-triplet separation, absorption spectral characteristics and room temperature solution phosphorescence of the Pd, Pt and Ru porphyrin make them extremely attractive sensitizers for use in studying photosensitized reactions and energy transfer processes. Metalloporphyrins with paramagnetic central metal ions show only phosphorescence with relatively short life times.

Table 1 : Luminescence properties of porphyrins at 300 K in solution.[a]

Non-luminescent	Fluorescence only	Phosphorescence only	Fluores. & Phosph.
Ni(II),VO,Sn(II)	Zn(II),Mg(II)	Co(III)	Pd(II)
Ru(II)L_2,Ru(III)	Sn(IV),Pb(II)	Rh(III),Ir	Pt(II)
Cu(II),Ag	Al,Cd,Free base		Ru(II)CO
Co(II)	Si(IV),Ge(IV)		
	Ba,Sr,Be		
	Sc(III), Ti(IV)		
	Zr(IV),Hf(IV)		
	Nb(V),Ta(V)		

a. From ref 9

Table 2 : Luminescence properties of porphyrins at low temperature in rigid medium[a].

Phosphorescence only	Phosphorescence and luminescence	Non-luminescent
Hg,Pb,VO	Pb,Pt,Ru,Mg,Zn	Ag
Mn(II),Fe(II)	Free base,Be,Ca,Sr	
Fe(III),Co(III)	Cd,Sn(IV),Ba,Sc(III)	
Ni,Cu,Ir	Ti(IV),Zr(IV),	
	Hf(IV),Nb(V),Ta(V)	

a. From ref 9

(c) Acid-Base Properties of porphyrins.

The free base porphyrin (PH_2) can add protons to its imine type (-N=) nitrogen atoms to form mono- (PH_3^+) or dications (PH_4^{2+}) or lose protons from its pyrrole type (-NH-) nitrogens to produce the mono (PH^-) or di-anions (P^{2-}). The proton dissociation equilibria are described by pK values as follows:

$$PH_4^{2+} \overset{pK_4}{\rightleftharpoons} PH_3^+ \overset{pK_3}{\rightleftharpoons} PH_2 \overset{pK_2}{\rightleftharpoons} PH^- \overset{pK_1}{\rightleftharpoons} P^{2-}$$

pK_1 and pK_2 refer to the acidic equilibria involved in the dissociation of protons from the pyrrole type nitrogens, and pK_3 and pK_4 refer to the basic equilibria associated with addition of protons to the imine type nitrogens. For H_2(TPP) the values of pK_3 and pK_4 are 4.4 and 3.9 respectively[12]. When three or four protons occupy the porphyrin central cavity, the strong Van der Waals and coulombic repulsions tend to distort the planarity of the porphyrin ring[13]. When the monocation (PH_3^+) is formed the pyrrole rings tilt alternately upwards and downwards with respect to the mean porphyrin plane. Such deformation facilitates protonation of the remaining lone pair, thus limiting the existence of the monocation. In the case of $H_4(TPP)^{2+}$ such distortion facilitates the rotation of phenyl rings which become nearly coplanar with the porphyrin ring, and lead to more extended conjugation. For this reason $H_4(TPP)^{2+}$ is more stable than alkyl-substituted porphyrins[14].

(d) Redox Chemistry .

The redox properties of metalloporphyrins have been studied extensively in view of the fact that they dominate the electron transfer processes of life. The initial focus and interest in the oxidation states of these systems stems from the redox properties of cytochromes (which are enzymes containing iron porphyrins and function catalytically via the Fe(II) $\rightleftharpoons$ Fe(III) couple) and the function of hemoglobin (an Fe(II) porphyrin which unlike simple Fe(II) porphyrins is not oxidized by oxygen to Fe(III) but reversibly binds oxygen at the Fe(II) oxidation level). The central role of iron in these naturally occuring systems led to the belief that the macrocyclic porphyrin ligand serves merely to modify the redox potentials of the metal, and to act as a convenient bridge between the metal and the protein. However, in 1964 when Closs and Closs isolated and characterized[15] the π-anion and π-dianion of ZnTPP, the ability of the porhyrin π-system to undergo redox reactions was fully apreciated.

The following scheme illustrates the redox reactions of porphyrins.

$$P^{2-} \rightleftharpoons P^{-} \rightleftharpoons P \rightleftharpoons P^{+} \rightleftharpoons P^{2+}$$

π-dianion; π-anion radical; Free base; π-cation radical; π-dication

The metalloporphyrins have low oxidation potentials[16-18](Table 3). The $E_{1/2}$ of the metallo-TPP's and H_2TPP is close to 1 volt. The 2^{nd} oxidation potential is about 0.3 volts higher. π-cation radicals of metalloporphyrins can be made quite easily by anodic oxidation in the presence of an appropriate electrolyte. Chemical oxidation by bromine or ceric ion, for example, is also easily achieved[19,20].

The porphyrin π-cation radicals have a characteristic green color. They have markedly reduced intensity of absorption in the visible region and the Soret bands are less intense and blue shifted by about 15 nm[21]. At room temperature the green solutions of π-cation radicals exhibit highly isotropic esr signals with a g value of approximately 2.00. Weak hyperfine splitting corresponding to nine lines could be seen on the esr spectrum of $ZnTPP^+$ ClO_4^- in butyronitrile at room temperature[22]. In the presence of oxygen the signal was broadened and the hyperfine structure was lost. Removal of oxygen regenerated the original nine lines. However, the esr spectrum of $MgOEP^+$ ClO_4^- was partially resolved to 5 lines. These results have indicated that π-cation radicals fall into two general categories. Depending on whether the electron is removed from a_{2u} or a_{1u} highest occupied orbital, the ground state configuration of the radical can be either $^2A_{2u}$ or $^2A_{1u}$ respectively.

Table 3 : Half-wave potentials of some metalloporphyrins[a]

Compound	Ring Oxidation[b]		Ring Reduction[c]	
	(2)	(1)	(1)	(2)
H_2TPP	1.28	0.95	-1.05	-1.47
Co(II)TPP	1.26	1.06	-1.87	
Cu(II)TPP	1.16	0.90	-1.20	-1.68
Fe(III)TPPCl		1.4	-1.65	
Fe(III)TPP		1.36		
Ru(II)TPPCO	1.21	0.82		
Zn(II)TPP	1.03	0.71	-1.35	-1.80

a. From ref [18]

b. Oxidations are in CH_2Cl_2 or butyronitrile

c. Reductions are in DMF or DMSO

Table 4 : Spin densities in porphyrin cation radicals[a]

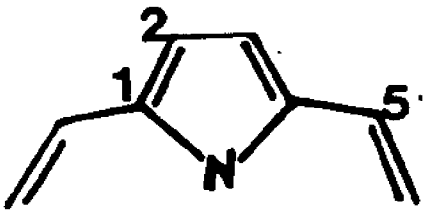

	$^2A_{2u}$ calculated	$^2A_{1u}$ calculated
C-1	-0.0094	0.0981
C-2	0.0134	0.0262
C-5	0.1932	0.000
N	0.049	0.000

a. From ref 23

In the $^2A_{2u}$ state the spin densities are high at meso carbon and nitrogen atoms while the $^2A_{1u}$ state has low spin densities at these atoms. In the latter state spin density is primarily confined to α-pyrrolic carbon atoms (Table 4) Therefore the nine hyperfine splitting lines in the $ZnTPP^+$ esr spectrum can be explained in terms of interations of the unpaired electron with four equivalent nitrogens (I=1) in $^2A_{2u}$ state. These assignments have been verified by deuterium substitution.

The esr spectrum of $ZnTPP^+$ cation radical has been found to be sensitive to the nature of the counter ion and the dielectric constant of the solvent[24]. Oxidation of ZnTPP by controlled-potential electrolysis in CH_2Cl_2 with $(C_3H_7)_4NClO_4$ as carrier electrolyte, results in a stable π-cation radical $ZnTPP^+ ClO_4^-$ with nine line esr spectrum. Chemical oxidation of ZnTPP in CH_2Cl_2 or $CHCl_3$ with 0.5 mol of Br_2 is reversible and produces a radical with the same absorption spectrum as $ZnTPP^+ ClO_4^-$, but with four line esr spectrum. The four line spectrum is thus assigned to hyperfine interation of the $ZnTPP^+$ radical with one Br^- (I=3/2).

In general, cation radicals of organic compounds are known to react with nucleophiles and also undergo electron transfer reactions[25]. Electron transfer reactions of π-cation radicals of porphyrins are biochemically important[26]. Due to extended conjugation of the porphyrin

π-ring, porphyrin π-cation radicals are known to be quite stable. π-cation radicals of ZnTPP has been found to be stable in nucleophilic solvents and isolated in crystalline form[20]. Reactions of ZnTPP cation radical perchlorate ($ZnTPP^{+}\ ClO_4^-$) with pyridine, triphenylphosphine, triphenylarsine, nitrite ion, thiocyanate ion, methanol, water, ammonia, methyl amine and dimethyl amine have been reported[27-29].

The reaction of nucleophiles such as methanol, water, acetate and halides with the $ZnTPP^{+}$ cation radical[28] or the $ZnTPP^{2+}$ dication[20], produces a dark green compound in which the nucleophile has added at the meso position, which has the structure [5-(methoxy)-5,10,15,20-tetrakis(pnenyl)porphinato]Zn(II) (10). Such a compound is also known as an isoporphyrin.

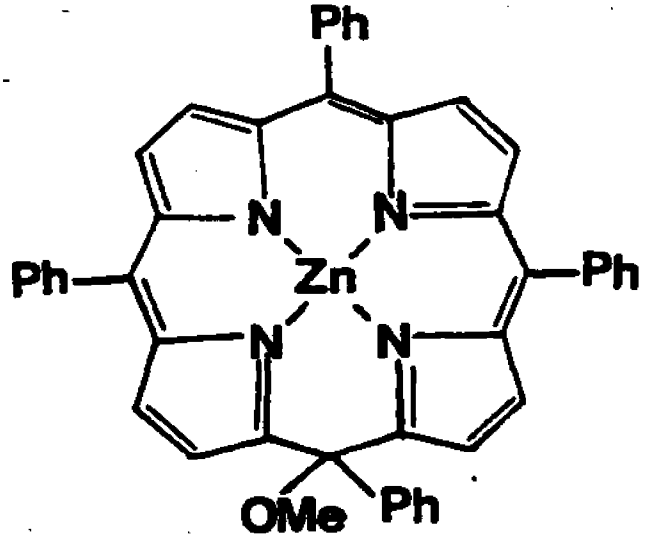

(10)

In isoporphyrins π-conjugation is disrupted at the meso position where the nucleophile has been added on. As a consequence of this the optical absorption spectrum changes dramatically. Fig. 21 shows the absorption spectrum of the isoporphyrin (10). In addition to the Soret band at 440 nm ($\epsilon \sim 4 \times 10^4$) which is less intense than the Soret band of ZnTPP ($\epsilon \sim 5 \times 10^5$, λ_{max}=410 nm) (see Fig. 1 on page 6), isoporphyrin absorption spectrum contains two absorption maxima towards near-IR region 780 nm, $\epsilon \sim 1.1 \times 10^4$ and 850 nm $\epsilon \sim 1.8 \times 10^4$). The positions and relative intensities of the near IR bands seem to be unique to isoporphyrins. UV-Vis spectra similar to the spectrum of Fig. 21 have been reported for the ferric isoporphyrins formed from the reaction of (meso-tetraphenylporphinato)-iron (III) complexes and cumene hydroperoxide or m-chloroperoxybenzoic acid[30,31] or from the reaction of TPP(p-OCH_3)FeCl and tert-butylhydroperoxide [32].

In the case of meso-tetraphenyl derivatives these isoporphyrins are stable and have been isolated and characterized[20] as the perchlorate salts. With octaethyl derivatives, however, the intermediate isoporphyrin can lose a proton to give the neutral meso-substituted metalloporphyrin[33]. This is because phenyl is a poor leaving group.

(e) Resonance Raman Spectroscopy.

Resonance Raman spectroscopy is a suitable analytical tool for porphyrins and metalloporphyrins because of their intense absorption bands in the visible and near ultraviolet regions. Raman spectra of hemoglobin were first reported in 1972[34,35]. Since then the RR spectra of a large number of porphyrins and its derivatives have been published.

One major problem encountered in RR studies of porphyrins is the high background due to fluorescence. Fortunately, Fe, Co, Ni and Cu porphyrins do not fluoresce or fluoresce extremely weakly. There are a number of methods of minimizing the effect of fluorescence. One of them is the use of quenchers. For those complexes that emit in solution, efficient quenching is noted in solid or KBr pellet samples. The other method is to use shorter wavelengths to avoid scanning into the fluorescent range. Due to high absorbance of incident radiation most porphyrins tend to decompose when exposed to a laser beam for extended periods of time. A sample rotation technique has proved to be useful in this respect. By defocusing the laser beam, sample overheating can be prevented.

As explained under absorption spectra the symmetry group of metalloporphyrins is D_{4h}, which gives rise to two excitations $a_{1u} \dashrightarrow e_g$ and $a_{2u} \dashrightarrow e_g$ which by configuration interaction produce a strong B band and weaker Q band. The RR spectra of metalloporphyrins have been

explained using this four orbital model[36,37]. These spectra are dominated by bands in the range 1100-1650 cm^{-1}, corresponding to stretching of the porphyrin-ring -bonds as expected for enhancement via $\pi - \pi^*$ transitions. Excitation near the Soret band enhances totally symmetric modes via A term scattering. With excitation in the Q_{0-0} and Q_{1-0} bands, the A term enhancement is much lower, because of the smaller electronic transition moment. The Q band RR spectra are generally dominated by the non-totally-symmetric modes responsible for Q-B mixing and the generation of the Q_{1-0} absorption. The bands of different symmetry can be identified by recording spectra with polarizer oriented such that the electric vector of the scattered radiation is parallel to the electric vector of the incident, linearly polarized radiation. Rotation of the polarizer by 90° affords the perpendicular spectrum with intensities $I_\perp$. The depolarization ratio is defined as

$$\rho = \frac{I_\perp}{I_{//}}$$

and is a characteristic of the molecular and vibrational symmetry. Raman lines for which $\rho < 3/4$ are denoted as polarized (p), $\rho = 3/4$ depolarized (dp) and $\rho = \infty$ inversely polarized (ip). In a molecule as complicated as a metalloporphyrin, polarized or depolarized vibrations which accidentally overlap an inversely polarized line will provide some intensity to $I_{//}$, making the value of ρ less than ∞. For those bands $3/4 < \rho < \infty$ are

called anomalously polarized (ap)[35].

According to the D_{4h} symmetry assigned to metalloporphyrins with H atoms at meso carbon atoms there can be 71 in-plane modes classified as

$$\text{in-plane} = 9\ A_{1g} + 8\ A_{2g} + 9\ B_{1g} + 9\ B_{2g} + 18\ E_u$$

There are 35 Raman active bands, nine of them polarized (A_{1g}), 18 depolarized (B_{1g} and B_{2g}) and 8 anomalosly polarized (A_{2g})

The out-of-plane vibrational modes are classified as:

$$\text{out-of-plane} = 3\ A_{1u} + 6\ A_{2u} + 4\ B_{2u} + 5\ B_{1u} + 8\ E_g$$

Only the eight E_g modes are Raman-active and their activation requires vibronic coupling between in and out of plane electronic transitions.

In TPP the RR spectrum contains more polarized bands than can be accounted for by the porphyrin skeleton. The polarized, relatively weak bands at 1599, 1030, 995 and 886 arise from modes that are internal to the phenyl rings[38]. Their resonance enhancement suggests significant conjugation of the phenyl rings with the porphyrin π system[39]. This conjugation refers only to the excited state, as in the ground state the large phenyl tilt angles and barrier to rotation by ortho hydrogen atoms prevents any conjugation.

The RR spectra have been reported for bacteriochlorophyll cation radicals[40,41]. Recently RR spectra of π -cation

radicals of Mg, Zn and Cu complexes of TPP in the 800-1800 cm^{-1} region were compared to spectra of MgTPP, ZnTPP and CuTPP[42]. Differences in intensities of bands and frequencies were observed. The phenyl modes were unaffected as expected. The frequency shifts were not large, and one to one correspondence was possible between the Raman bands of the radical and those of the corresponding metalloporphyrins. Those frequency shifts were explained in terms of the electronic structure in the ground state of the metalloporphyrins and their cation radicals.

(f). Metalloporphyrins as Catalysts.

Perhaps the best known catalysts are the protein enzymes which are known to catalyze nearly all chemical reactions in living cells. Nearly a million fold or more rate enhancements have been observed when such reactions are catalyzed by enzymes. Furthermore enzymes display a remarkable specificity which extends to particular stereoisomeric forms. However, many metabolic reactions cannot be catalyzed alone by the amino acid side chain functional groups of the enzymes. Enzyme catalysis of most of the reactions are performed in cooporation with coenzymes. Examples of coenzymes are heme coenzymes, iron-sulfur clusters, flavin coenzymes and nicotinamide coenzymes. In heme coenzymes chelation of the dianionic form of protoporphyrin IX, one of the most commonly occuring of a number of porphyrin structural variants, with an iron atom produces protoheme IX (11).

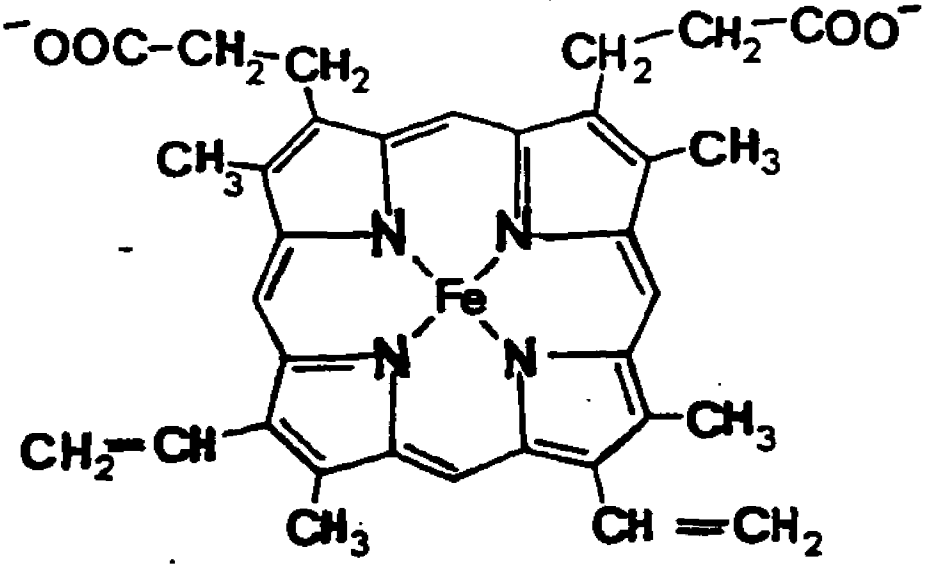

(11)

Examples of protein molecules that incorporate heme prosthetic groups are hemoglobin, myoglobin and cytochromes. Although all these molecules share a common prosthetic group they have different properties and serve different purposes, according to the type of interactions between the heme and the polypeptide chain. For example, heme iron in myoglobin reversibly binds oxygen without itself becoming oxidized. In contrast, the heme iron in cytochrome c is reversibly oxidized and reduced between Fe^{2+} and Fe^{3+}. Cytochrome P450, named for the wavelength corresponding to the most intense absorption band of the carbon monoxide liganded heme, is the heme protein in multienzyme systems that catalyze the hydroxylations of hydrocarbons such as steroids. Very few chemical systems are known to efficiently catalyze alkane hydroxylation under such mild conditions[44]. FeTPPCl has been successfully used to catalyze the hydroxylation and epoxidation of nonactivated C-H bonds with iodosylbenzene as the oxygen source[43]. A review of use of metalloporphyrins as catalysts for dioxygen reduction and p-450 type hydroxylations has appeared [45]. Table 5 compares various metalloporphyrins as catalysts for the oxidation of cyclohexane with cumyl hydroperoxide $C_6H_5C(CH_3)_2OOH$ as the oxygen source.

Table 5 : Cyclohexane oxidation by cumyl hydroperoxide with various catalysts[a]

Catalyst	FeTPPCl	$TPPH_2$ or $FeCl_3$ or $FeCl_2$	Co(II)TPP	M(II)TPP M=Cu,Ni,Zn or Mg	M(IV)(TPP)O M=Ti, V	M(III)TPPCl	OsTPP(CO)Py
Yield(%)							
After 15 min							
Cyclohexanol	40	0	45	0	0 (25 after 10 days)	1	5
Cyclohexanone	20	0	23	0	0 (12 after 10 days)	0.5	2.5
$t_{1/2}$ of $C_6H_5C(CH_3)_2$-OOH	1-2 min		0.3 min		3 days		3.5 hrs

a. From ref 47

From these results the metalloporphyrins studied can be divided into three classes. (i) The Cu(II), Ni(II), Zn(II), Mg(II), V(IV) and Ti(IV) porphyrins are completely inactive, (ii) CoTPP and Os(TPP)(CO)Py are able to catalyze cyclohexane oxidation but appear greatly modified at the end of the reaction, exhibiting decreased reactivity upon further hydroperoxide addition to the reaction mixture, (iii) Fe and Mn(III)(TPP)Cl are true catalysts found unchanged at the end of the reaction and exhibit a constant reactivity when new hydroperoxide is added. catalytic oxidations of organic substrates by metalloporphyrins of the following transition metals have been reported. Fe[46-50], Mn[51-55], Cr[56].

Metalloporphyrins have been used to catalyze other reactions in addition to hydroxylations[57-64]. Of particular interest to us was the catalytic decarbonylation of aldehydes using Ru(II)porphyrin systems[65,66]. Several aldehydes were catalytically converted to the corresponding hydrocarbon using a $Ru(TPP)(PPh_3)_2/^nBu_3P$ catalyst system.

The exact mechanism of this reaction has not been elucidated[66]. However, initial rapid dissociation of one of the PPh_3 groups at low concentrations of the complex appears to form a pentacoordinated species that adds a carbonyl group rapidly from gaseous CO or less rapidly from an aldehyde.

$$Ru(TPP)(PPh_3)_2 \rightleftharpoons Ru(TPP)(PPh_3) + PPh_3$$

$$Ru(TPP)(PPh_3) + \underset{\text{aldehyde}}{RCHO} \rightleftharpoons Ru(TPP)(CO)(PPh_3) + \underset{\text{alkane}}{RH}$$

It is not clear how the catalytic species is regenerated. Complexation of $^{n}Ru_3P$ with displacement of CO has been suggested as a possibility.

$$Ru(TPP)(CO)(PPh_3) + {}^{n}Bu_3P \rightleftharpoons \begin{cases} Ru(TPP)(CO)({}^{n}Bu_3P) + PPh_3 \\ Ru(TPP)({}^{n}Bu_3P)(PPh_3) + CO \end{cases}$$

D. POROUS VYCOR GLASS AS A SOLID SUPPORT.

(a) Properties of porous Vycor glass.

Porous Vycor glass (PVG), Corning code 7930, is nearly a pure form of silica with a small amount of boric oxide. It is made by acid leaching borosilicate glass[67]. Table 6 lists the composition and properties of PVG[68].

PVG is a good solid support because it is strong, chemically inert, thermally stable and it provides rapid activation and high adsorption. It is supplied in various shapes such as plates (of varying thickness), tubing, disks, fibers or granules. It is opalescent in appearence. On standing in atmosphere it absorbs organic matter from air and turns yellow. As described below under Raman studies, it is necessary to pretreat PVG before using as a solid support.

The Table (7) compares the properties of PVG with similar adsorbents[69]. A definite advantage of PVG over other adsorbents compared is its physical strength and transparency to visible light which makes it possible to be used for absorption spectroscopic studies. Absorption spectra can be recorded to ca. 240 nm relative to an untreated piece of PVG[70].

Table 6 : The Composition and Properties of porous Vycor glass.[a]

	Percentage Composition
SiO_2	96.3
B_2O_3	2.95
Na_2O	0.04
$R_2O_3 + RO_2$	0.72
Apparent Density (dry) gm/cc	1.5
Void Space % of vol	28
Average Pore Diameter, nm	70
Internal Surface Area, m^2/gm	200
Appearence	opalescent

a. From ref 68

Table 7 : Adsorbent materials and their properties[a]

Adsorbent	Composition and physical appearence	Pretreatment °C	Surface area (m^2/g)
PVG	96.3 % SiO_2, 2.9 % B_2O_3 1 mm plates	500 800	170 130
Silica gel	SiO_2 ~20 mesh powder	500	570
Silica-Alumina	28.6% Al_2O_3, 71.1% SiO_2 ~60 μmϕ particles	500 800	510
γ-Alumina	99.99% Al_2O_3 3.8 μmϕ particles	500	110

a. From ref 69

(b) Use of PVG for IR and Resonance Raman studies.

IR spectra of pyridine adsorbed on PVG have indicated the shift of pyridine bands in the C-H region due to the hydrogen bonding to the surface SiOH and BOH groups via the ring N atom[71].

Although PVG is a good solid support for resonance Raman spectroscopy, a piece of PVG that had been in contact with ambient air for several months and had become yellow shows strong fluorescence. Heating PVG in air or oxygen this fluorescence could be completely eliminated[72]. The Raman spectrum of clean PVG indicates a strong band at 3750 cm^{-1} assigned to OH stretching vibration[73]. Unlike the corresponding band in the IR it is comparatively weak and cannot be resolved into components corresponding to SiOH and BOH. It does not change with adsorption of substances. The Raman spectrum of water condensed in pores of a cleaned PVG sample rod was found to be identical with that of water in the bulk in the region of 1000-4000 cm^{-1},[73]. Both spectra contained a strong band at 3440 cm^{-1} and a weak band at 1645 cm^{-1}

(c) Cation radicals on PVG

Cation radicals can be made when aromatic and some olefinic molecules are deposited on solid surface of silica-alumina or alumina[25]. These types of catalysts are used for large scale hydrocarbon conversions in the petroleum industry and therefore the formation of cation radicals on such surfaces was, at one time, a subject of considerable interest. The catalyst has to be activated by heating in a current of air or oxygen for several hours before deposition of substrate.

Although PVG does not belong to the above mentioned categories of supports, it is known to produce cation radicals, at least in a few cases. When methyl iodide was adsorbed on PVG (pretreated at 600° to 650° in oxygen and cooled to room temperature in helium) and the sample was irradiated with a low-pressure mercury lamp, methyl radical was obtained[74,85]. The radical was stable for days in the PVG matrix.

1,1-diphenylethylene (DPE), when adsorbed on PVG undergoes spontaneous oxidation to produce a cation radical[75-78]. The question arises: where on the surface of PVG does the cation radical formation occur? The surface of PVG is considered to contain two types of acidic sites, Lewis and Bronsted. The one electron oxidation probably occurs at a Lewis acid site which may be a boron atom. There is no knowledge, however, about the fate of the

abstracted electron. It has been suggested that the electron deposited initially at each site is spread over the surface or within the crystal lattice of the catalyst so that the esr signal becomes broadened and undetectable[79]. There is some evidence that molecular oxygen may be the true electron acceptor.

The following scheme illustrates the reaction of DPE at the two different acid sites.

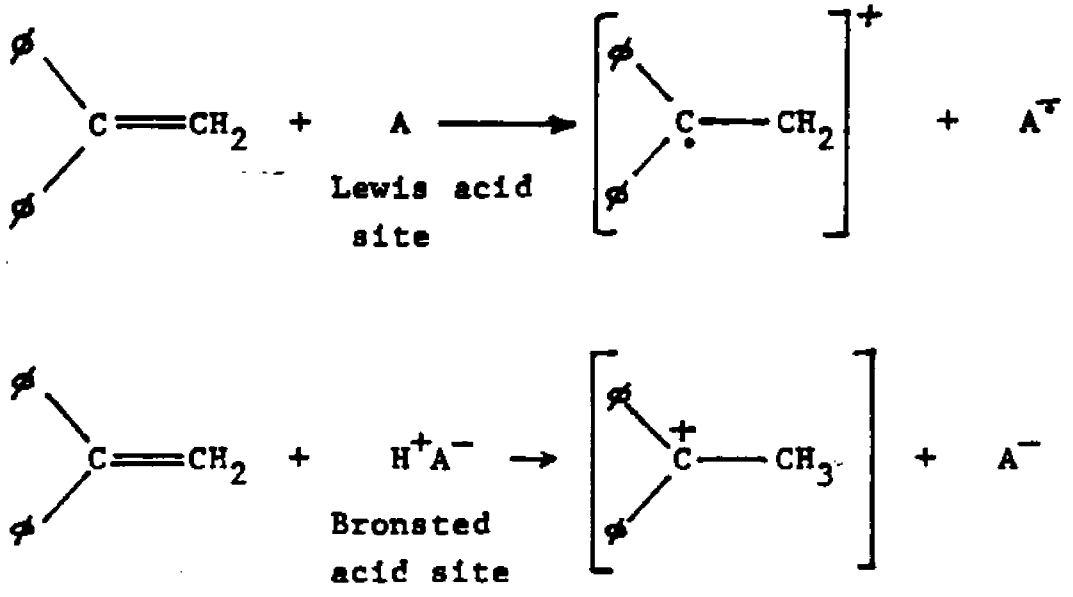

E. THE OBJECTIVE

Our initial goal was to evaluate the possibility of using PVG as a solid support for catalytically active metalloporphyrins. We chose to study the $RuTPP(PPh_3)(CO)$ catalyzed decarbonylation of aldehydes on PVG. Since the initial step of adsorbing a metalloporphyrin onto the PVG surface was not at all straightforward, what has evolved is a study of the interaction of various types of porphyrins and metalloporphyrins such as TPP, ZnTPP and RuTPP(CO) with the PVG substrate.

2. EXPERIMENTAL

A. MATERIALS

5,10,15,20-Tetraphenylporphyrin (H_2TPP) and Ru(TPP)CO were purchased from Man-Win Chemicals and used without further purification. Some Ru(TPP)CO used was also prepared starting from $Ru_3(CO)_{12}$ and H_2TPP[80,81,82]. ZnTPP was prepared from Zinc Acetate and H_2TPP[83]. The products were purified by chromatography on alumina grade III with CH_2Cl_2 as the eluent. All solvents used were spectroquality. For decarbonylation reactions aldehydes were distilled prior to use and stored under argon at 0°C. Phenylacetaldehyde and n-tributylphosphine were purchased from Alpha Chemicals and were stored in refrigerator under argon.

B PRETREATMENT OF PVG AND ADSORPTION FROM SOLUTION.

PVG was obtained from Corning Glass works in the form of plates of thicknesses 1mm and 4mm. The glass plates were cut on a carbide saw into approximately 25mm x 25mm pieces. The pieces of PVG were then extracted in a soxhlet extractor with distilled water and acetone to remove any adhering surface contaminants and water soluble materials. The extraction was usually carried out for about 24 hours. The pieces were then placed in a vacuum oven heated to about 150°C for about 3 hours to remove the bulk of the solvent adsorbed. Finally they were heated in a muffle furnace at

550°C for about 3 days, at atmospheric pressure. This procedure removed most of the carbonaceous impurities that cause high fluorescence in untreated PVG[72,73]. After that pieces of PVG were removed from the furnace and allowed to cool to room temperature in a vacuum desiccator. They were stored in the dessicator until used. Absorption of porphyrins and metalloporphyrins on PVG was carried out as follows[70,84,85]. A solution of the porphyrin was first made in a suitable solvent. The solvent frequently employed was methylene chloride. The concentration of the solution had to be such that the optimum amount of material adsorbed on PVG would allow spectroscopic studies. Approximately 10^{-5} M solutions were found to be suitable. The piece of PVG is then immersed in a portion of the solution and allowed to remain for about one half hour. The piece of PVG is then taken out and immediately put in a glass cell made to hold a piece of PVG vertically and steady inside a rectangular glass tube slightly bigger than the piece of PVG. When the glass cell is connected to the vacuum line the piece first becomes turbid when the solvent starts to evaporate and finally becomes clear when all the solvent had been removed. It is normally allowed to remain longer on the vacuum line to extract any trace amounts of solvents left on the piece of PVG.

C. INSTRUMENTATION.

(a) Absorption Spectra.

Absorption spectra were recorded on a Cary 14 or Perkin-Elmer Lambda 3 UV-Visible spectrophotometer. Some modifications of the sample compartment and sample holder were necessary to accomodate the special sample cell described earlier. A box made of plastic sheet and painted in black and made to properly seal with the sample compartment cavity was used instead of the compartment cover.

(b) Emission Spectra.

Emission spectra were recorded on a Perkin-Elmer Hitachi MPF-2A spectrophotometer equipped with a red sensitive Hamamatsu R818 photomultiplier tube. For low temperature emission spectra, solutions in 2mm-i.d. quartz tubes were placed in a quartz Dewar filled with liquid nitrogen. As for absorption spectra the sample compartment cover had to be replaced with a lightproof box to accomodate the special cell. When recording the emission spectra of adsorbed compounds the piece of PVG had to be oriented such that the excitation radiation was not directly reflected on to the photomultiplier tube.

The Raman spectrometer (described below) was sometimes

used to record emission spectra. The advantages of this method were a) the red sensitivity of the photomultiplier tube of the Raman spectrometer was higher, (it was possible to record emission spectra up to 850 nm) b) higher resolution of emission bands c) higher intesity of otherwise weaker bands. The main disadvantage of this method was the sample decomposition under intense laser beam.

c) Resonance Raman Spectra.

The main components of the Raman spectrometer are[86] (see fig 2)

(1) Spex model 14018 double monochromator with holographiclly ruled gratings,

(2) RCA C31034A photomultiplier tube having extremely high cathode resposivity and UV transparent glass window. Dark noise reduced by cooling to about -20^{o}C using Pacific Precision Instruments phototube housing.

(3) Pacific Precision Instruments model 126 laboratory photometer for photon counting.

(4) Spectra Physics 164-08 argon ion continuous wave laser and a Coherent 590 dye laser.

(5) An Apple computer interfaced with the photometer and wavenumber drive of the monochromator. The spectra were routinely recorded and stored on floppy disks.

Figure 2 : The components of the Raman Spectrometer.

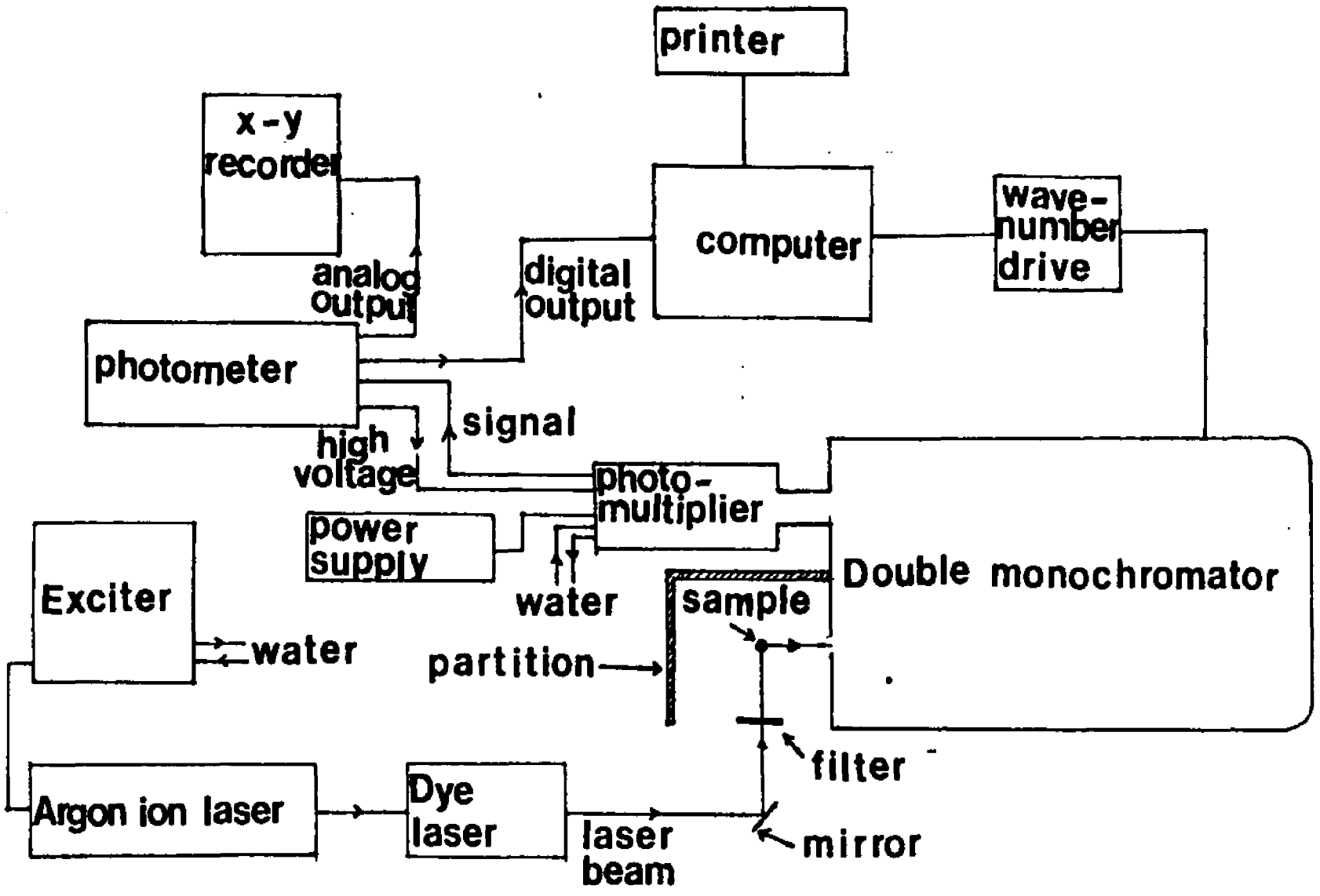
printer
x-y recorder
computer
wave-number drive
analog output
digital output
photometer
signal
high voltage
photo-multiplier
power supply
water
Double monochromator
sample
Exciter
water
partition
filter
Argon ion laser
Dye laser
laser beam
mirror

d) Electron Spin Resonance Spectra.

The ESR spectrometer was a Brucker ER 200E - SRC electron spin resonance spectrometer with Brucker ER 081(90/30 C 5) reflex klystron as microwave source and Brucker ER 041 MR as the microwave bridge. The ESR spectrometer was interfaced with an apple computer which was used in combination with "Acquire" data acquisition system, to record and save spectra on floppy disks.

D. MEASUREMENT OF SURFACE PH OF PVG

The most common and satisfactory procedure for measuring pH values by means of indicators is termed the Sorensen method. Equal amounts of a suitable indicator solution are added to equal volumes of the unknown and of one or more reference solutions of known pH. The colors of solutions are then compared using a spectrophotometer. The pH of the unknown is obtained by matching the absorption maxima. It is possible to apply such a method to measure the surface pH of PVG as it is transparent to visible light. First a few drops of the indicator solution is applied to both surfaces of a piece of PVG and allowed to stand for about 3 minutes, so that the dye will spread evenly on the surfaces. This piece of PVG is then mounted in the glass cell described earlier and placed in the specrophotometer. The absorption spectrum of this piece is then recorded in the visible region with a clean piece of PVG in the reference compartment.

Buffer solutions with their pH's differing by .5 pH units were prepared using potassium hydrogen phthalate and standard HCl or standard NaOH solutions (Table 8)[87]. The pH values of the buffer solutions were checked before use in the experiment but the variation was not greater than $\pm$ 0.1 pH units, from the theoretical value . The indicators used and their pH ranges and color changes are given in Table 9

Table 8 : Preparation of buffer solutions and their pH values.

50 ml 0.1 M KHphthalate + x ml 0.1 M HCl, diluted to 100 ml.		50 ml 0.1 M KHphthalate + x ml 0.1 M NaOH, diluted to 100 ml	
x	pH	x	pH
38.8	2.5	8.7	4.5
22.3	3.0	22.6	5.0
8.2	3.5	36.6	5.5
0.1	4.0	43.7	6.0

Table 9 : Indicators used, their transition pH ranges and the corresponding color changes.

Common Name	Transition range(pH)[a]	Color Change	
		acid	base
Cresol Red	0.4 - 1.8	red	yellow
Cresol Red[b]	7.0 - 8.8	yellow	red
Thymol Blue	1.2 - 2.8	red	yellow
Thymol Blue[b]	8.0 - 9.6	yellow	blue
Bromocresol Green	3.8 - 5.4	yellow	blue
Methyl Red	4.8 - 6.0	red	yellow

a) From Handbook of Chemistry and Physics, CRC press, Inc.

b) Indicator has a dual pH range.

E. CONTROL EXPEIMENTS IN OXYGEN FREE ATMOSPHERE

Surface adsorbed oxygen on PVG was removed by connecting a powdered sample to a vacuum line of pressure 10^{-3} torr. Samples of PVG were also prepared by heating in a sand bath up to 150°C, while being connected to vacuum line.

For adsorption of metalloporphyrins from solutions a glove box was used. The glove box was initially purged with argon pumped through Fieser's solution to remove any traces of oxygen. Fieser's solution was made by dissolving 2g of sodium anthraquinone β-sulfonate in 100 ml of 20% (w/v) KOH solution and then adding 15g of sodium dithionite. The solution appeared red when fresh and turned white when reacted with oxygen. The porphyrin solution was made oxygen free by bubbling argon through it inside the glove box. The PVG sample is opened inside the glove box and immediately immersed in the porphyrin solution. After about 15 minutes when the adsorption is complete the tube is closed inside the glove box and transferred to the vacuum line, where the solvent is removed.

The interior of the glove box although oxygen free remained saturated with water vapor as argon was pumped through the Fieser's solution which contained water as the solvent.

F. DECARBONYLATION REACTIONS

$Ru(TPP)(PPh_3)$ was prepared from Ru(TPP)CO using the following procedure[80,88]. 1 mmol of Ru(TPP)CO partially dissoved in CH_2Cl_2 (50 ml) was treated under nitrogen with an excess of PPh_3 ligand (3 mmol) under magnetic stirring. An immediate evolution of CO occurs and after 1 hr the crude product is precipitated by dilution with CH_3OH. It was purified using a column filled with acidic alumina with benzene-CH_2Cl_2 as the eluant.

The decarbonylation was carried out using the procedure described[65]. 10^{-1} mmol of $Ru(TPP)(PPh_3)_2$ was dissolved in 1 ml of CH_2Cl_2 and this was added to about 50 ml of acetonitrile containing the aldehyde (benzaldehyde or phenylacetaldehyde) (upto 0.5 M) and Bu_3^nP (phosphine:Ru approx 10:1). The system was activated by stirring under 1 atm of CO for a few seconds. CO was then replaced by argon while the reaction took place. The products were monitored on a Varian model 1400 gas chromatograph with a 6 ft steel column packed with Chromosorb 101 (purchased from Supelco, Inc.) The column was heated to about 150^o.

3. RESULTS

(A) MEASUREMENT OF SURFACE PH OF PVG

When the indicators mentioned in table 9 were adsorbed on PVG the color changes described in table 10 were observed. The color changes in these indicator solutions suggest a value of 2.8-3.8 for the pH of PVG.. For this reason buffer solutions having pH values close to this value and differing by 0.5 pH units were used with indicators cresol red and bromocresol green that have transition ranges at low pH values. The absorption maxima and their optical density values obtained with buffer solutions are compared with those obtained with PVG in tables 11 and 12 for indicators cresol red and bromocresol green respectively.

Table 10 : Color changes observed when the indicator was applied to a piece of PVG.

Indicator	Color in PVG
Cresol Red	yellow
Thymol Blue	yellow
Bromocresol Green	yellow
Methyl Red	red

Table 11: Spectroscopic absorption maxima observed for Cresol Red in the buffer solutions and in PVG.

pH	O.D.(1)[a]	O.D.(2)[b]	O.D.(2)/O.D.(1)
4.0	0.26	0	0
3.5	0.42	0	0
3.0	0.46	0.06	0.13
2.5	0.26	0.235	0.90
PVG	2.0	0	0

a) Optical density at 432 nm.

b) Optical density at 520 nm.

Table 12 : Spectroscopic absorption maxima observed for Bromocresol Green in the buffer solutions and in PVG

pH	O.D.(1)[a]	O.D.(2)[b]	O.D.(1)/O.D.(2)
5.9	0.24	0.07	3.43
5.5	0.22	0.07	3.14
5.0	0.16	0.055	2.91
4.5	0.085	0.065	1.31
4.0	0.035	0.1	0.35
3.5	0	0.11	0

a) Optical density at 615 nm

b) Optical density at 440 nm

(B). ABSORPTION, EMISSION, RESONANCE RAMAN AND ELECTRON SPIN RESONANCE SPECTROSCOPIC STUDIES.

(a) TPP

Porphyrins and metalloporphyrins form purple solutions in methylene chloride. Free base meso-tetraphenylporphyrin (H_2TPP) shows a spectrum with an intense Soret band at 416 and four bands in the visible region at 514, 548, 590 and 646 with decreasing intensity (Fig. 3). When the free base is adsorbed on PVG the color of the piece of PVG immediately turns green. Before the absorption spectrum of H_2TPP adsorbed on PVG is recorded, the solvent is removed in vacuo. The piece of PVG first becomes turbid when the solvent starts to evaporate and when all the solvent has been removed appears clear green. There are three major differences between the absorption spectra of TPP(adsorbed) (Fig. 4) and TPP(solution) (Fig. 3). First there is an extra Soret band in the adsorbed species at 450 nm. Second, the intensity ratio of the four visible bands are different from that in solution spectrum. The bands at 512 nm and 660 nm have almost equal intensities, where as in the solution spectrum the 514 nm band is much more intense than the band at 646 nm. The third difference is that the 660 nm band of the adsorbed spectrum is 14 nm red shifted compared to 646 nm band. The emission spectrum of the TPP(adsorbed) is very much different from the emission spectrum of TPP(solution) (Fig. 5). The emission spectrum in solution consists of 2 bands at 650 nm and 718 nm whereas the emission of

TPP(adsorbed) consists of strong emission at 680 nm.

The resonance Raman spectra of TPP(solid) (Fig. 6) and TPP(adsorbed) (Fig. 7) were obtained using the excitation wavelength 457.9 nm. As shown in the absorption spectra (Fig. 3 and 4) the resonance enhancement of the adsorbed compound is much higher because the wavelength of excitation falls within the Soret band. Comparison of the RR spectra reveals similarities as well as differences (Table 13). There is a change in the frequency of the major band at 1551 cm^{-1} of TPP(solid) by about 5 wavenumbers to 1546 in the TPP(adsorbed). The weak 1440 cm^{-1} band of TPP(solid) and weak 1475 cm^{-1} band of TPP(adsorbed) are too far apart to be the same band. The 1294 cm^{-1} band of TPP(solid) and 711 band of TPP(adsorbed) do not have corresponding bands .

The epr spectrum of TPP adsorbed was taken after depositing on PVG powder from 5 X 10^{-5} M solution in air and solvent removed in vacuo. The spectrum at room temperature in vacuum is given in Fig. 8. The g value calculated is 2.00, and peak-to-peak first derivative width (ΔH_{ptp}) is 3.5 G. No hyperfine structure was seen on the signal. The signal disappeared when air was introduced into the epr tube but reappeared when reevacuated.

Fig. 9 and Fig. 10 show the absorption and emission spectra of TPP in glacial acetic acid. As shown in the absorption spectrum the wavelength of excitation used for the resonance Raman spectrum falls directly within the Soret

band, which gives rise to strong resonance Raman bands (Fig. 11) The resonance Raman bands in this spectrum are compared to the bands in the RR spectra of TPP(solid) and TPP(adsorbed) in Table 13. It is interesting to note that the strongest band at 1546 cm^{-1} shows the downward shift of 5 cm^{-1} similar to that in TPP(adsorbed) from TPP(solid). The 1475 cm^{-1} band of TPP(adsorbed) correspond to 1478 cm^{-1} band of TPP(acetic acid). Similarly 711 cm^{-1} band of TPP(adsorbed) corresponds to the 701 cm^{-1} band of TPP(acetic acid). Both these bands do not have corresponding bands in TPP(solid).

Another interesting point is that in acetic acid the emission occurs at the same wavelength as in TPP(adsorbed). This leads to a strong possibility that some TPP undergoes diprotonation when adsorbed onto PVG.

Figure 3: Absorption spectrum of meso-tetraphenyl porphyrin in methylene chloride solution (5×10^{-5} M solution, Soret region 1 mm cell, other 10 mm cell) The arrow marks the excitation wavelength used for the resonance Raman spectrum in Figure 6.

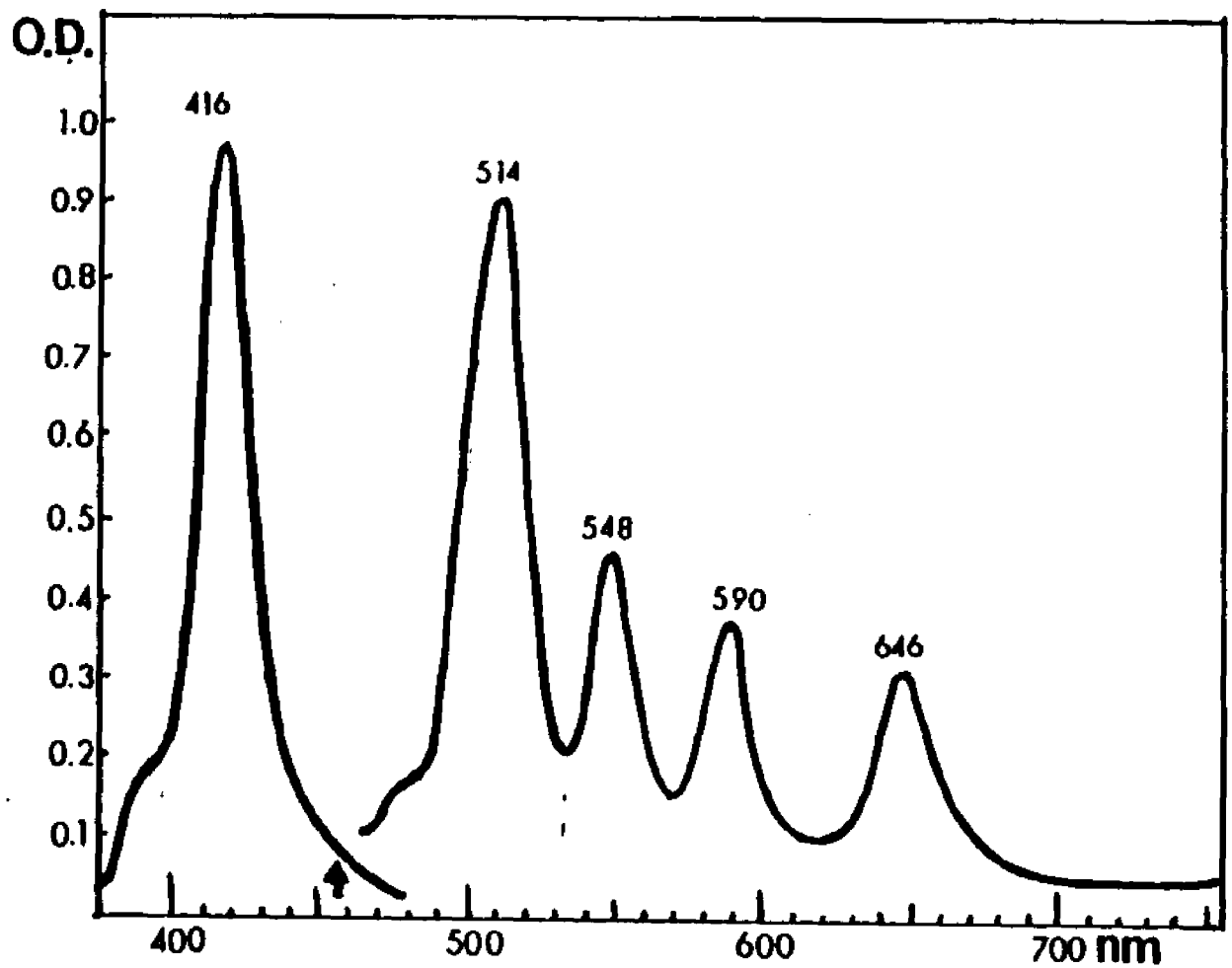
O.D.
1.0
0.9
0.8
0.7
0.6
0.5
0.4
0.3
0.2
0.1
416
514
548
590
646
400
500
600
700 nm
WAVELENGTH

Figure 4 : Absorption spectrum of meso-tetraphenyl porphyrin adsorbed on PVG. (10^{-8} moles adsorbed on a piece of PVG 25 mm x 25 mm x 4 mm) The arrow marks the excitation wavelength used for the resonance Raman spectrum in Figure 7.

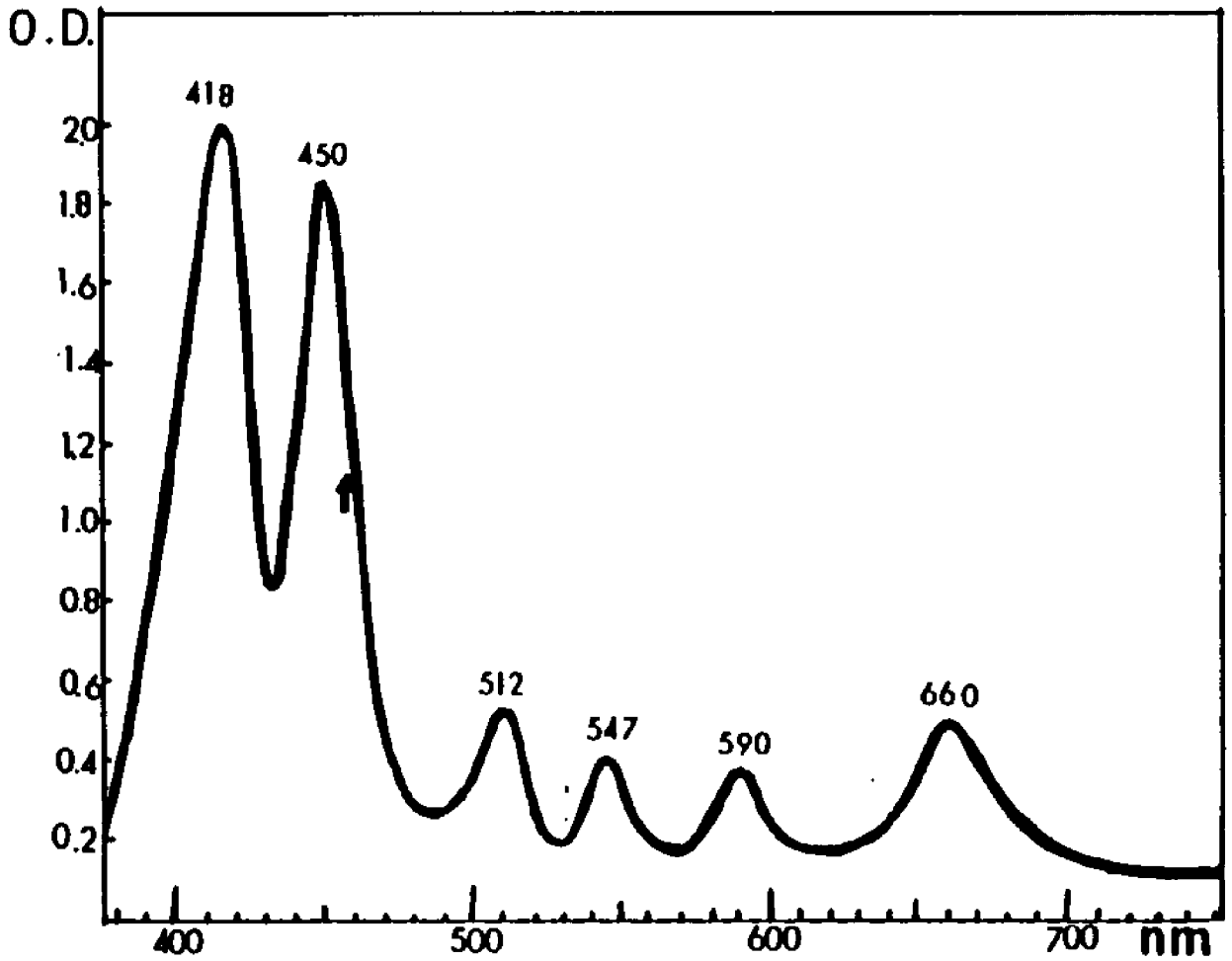
O.D.
2.0
1.8
1.6
1.4
1.2
1.0
0.8
0.6
0.4
0.2
418
450
512
547
590
660
400
500
600
700
nm

WAVELENGTH

Figure 5 : Emission spectra of meso-tetraphenyl porphyrin at 25°C. (a) Adsorbed on PVG (b) In methylene chloride solution. Wavelength of excitation = 410 nm.

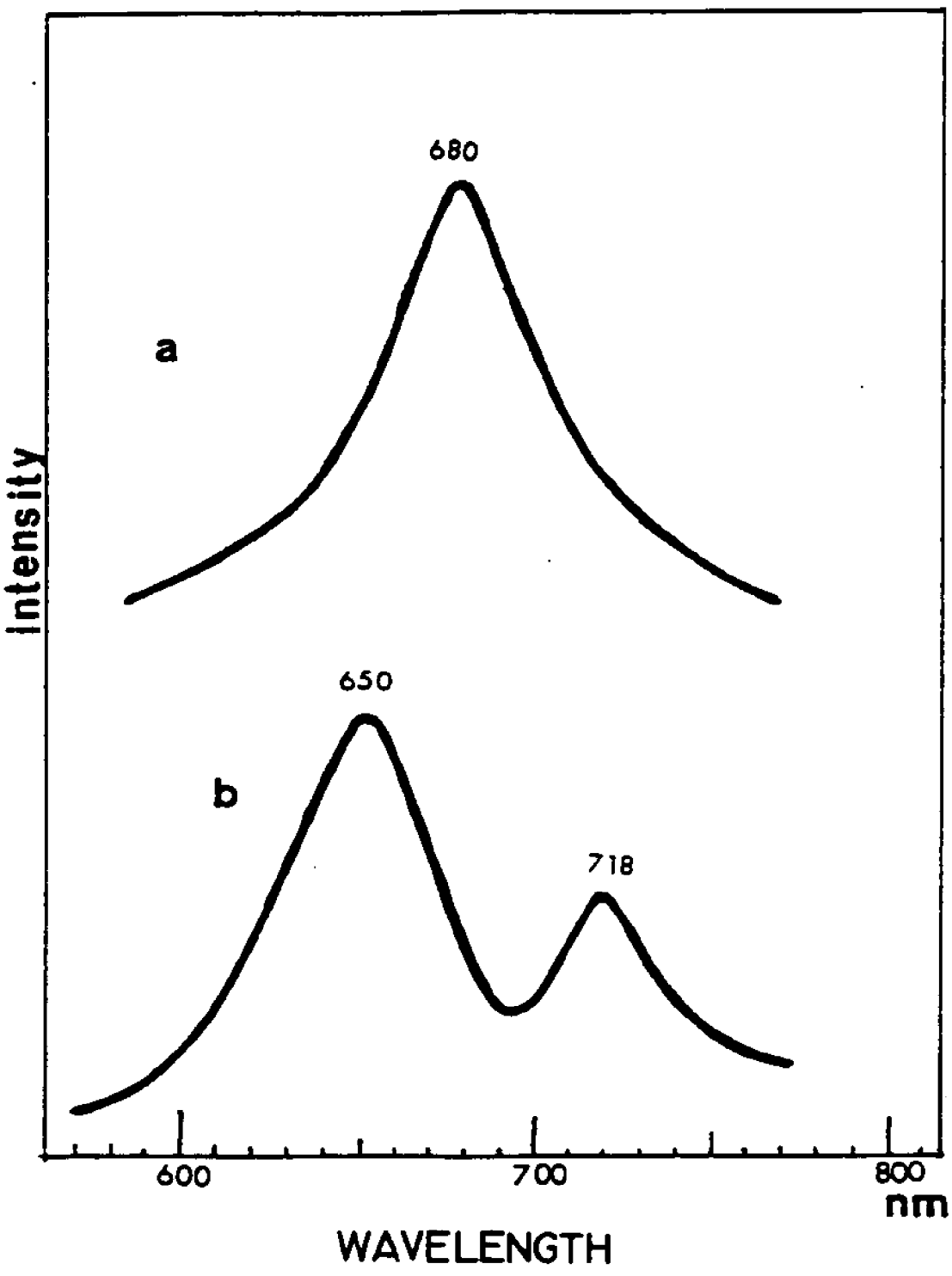
680
a
Intensity
650
b
718
600
700
800
nm
WAVELENGTH

Figure 6 : Resonance Raman spectrum of solid TPP mixed with KBr at room temperature. Excitation wavelength 457.9 nm (ca. 50 mW). Approximate spectral slit width 5 cm^{-1}. The spectrum was corrected for luminescence.

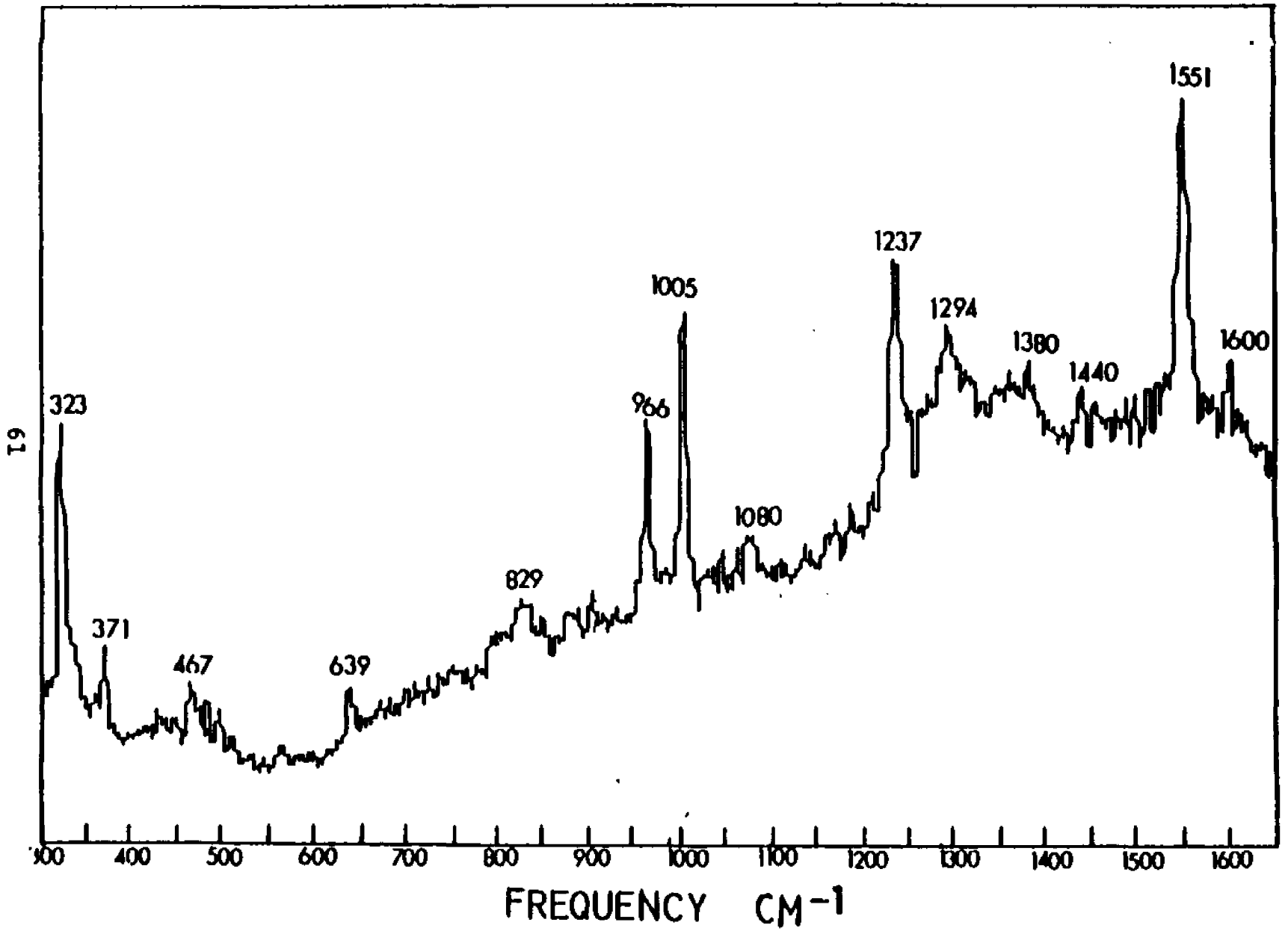
323
371
467
639
829
966
1005
1080
1237
1294
1380
1440
1551
1600
61
900
400
500
600
700
800
900
1000
1100
1200
1300
1400
1500
1600
FREQUENCY CM-1

Figure 7 : Resonance Raman spectrum of TPP adsorbed on PVG. Excitation wavelength 457.9 nm (ca. 30 mW) Approximate spectral slit width 5 cm^{-1}. The laser beam was defocussed to avoid sample decay. The spectrum was recorded at room temperature, in air and was corrected for luminescence.

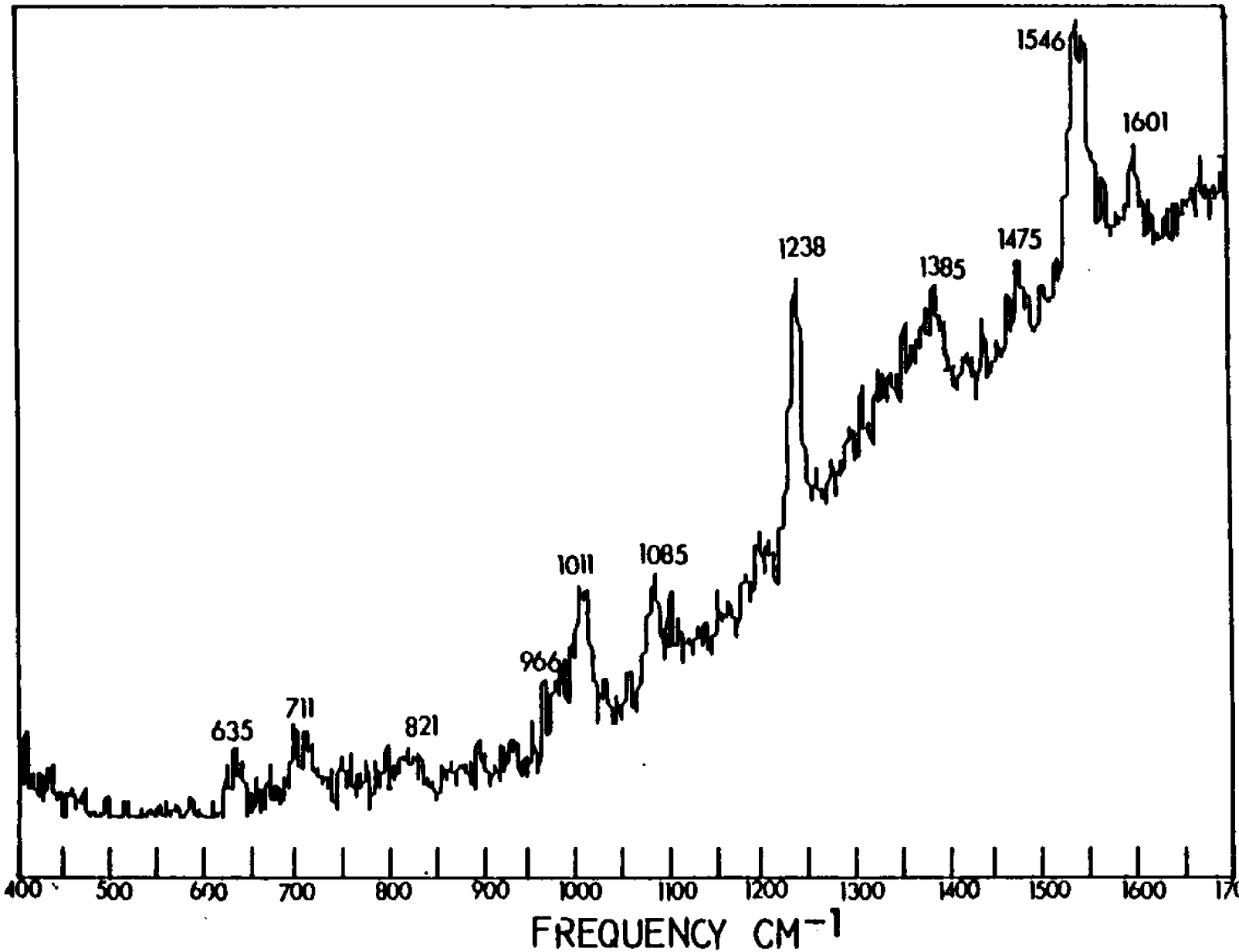
1546
1601
1238
1475
1385
1011
1085
966
635
711
821
400
500
600
700
800
900
1000
1100
1200
1300
1400
1500
1600
1700
FREQUENCY CM⁻¹

Figure 8 : Electron paramagnetic resonance spectrum, at 9.67 GHz, of TPP adsorbed onto powdered PVG, then evacuated. Spectrum was obtained with 20.2 mW microwave power using 100 kHz modulation (0.5 Gpp) and a gain of 10×10^5.

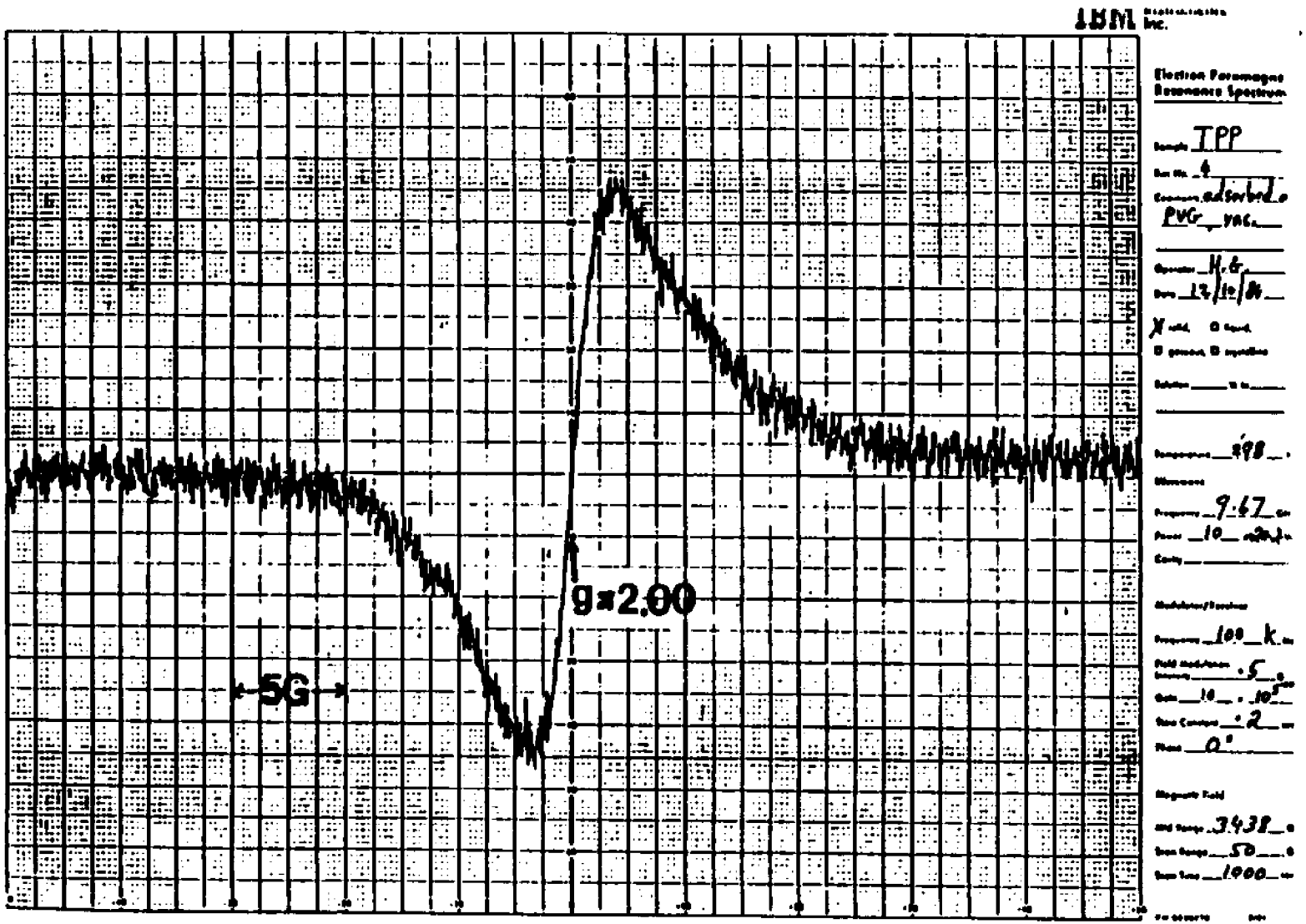
IBM Inc.
Electron Paramagnetic Resonance Spectrum
TPP
adsorbed
PVC vac.
H. G.
12/12/84
298
9.67
100 k
.5
10 . 10⁵
.2
0°
3438
50
1000
g=2.00
5G

Figure 9 : Absorption spectrum of TPP dissolved in glacial acetic acid. (10^{-6} M solution, Soret region 1 mm cell, other 10mm cell) The arrow marks the excitation wavelength used for the resonance Raman spectrum in Figure 11.

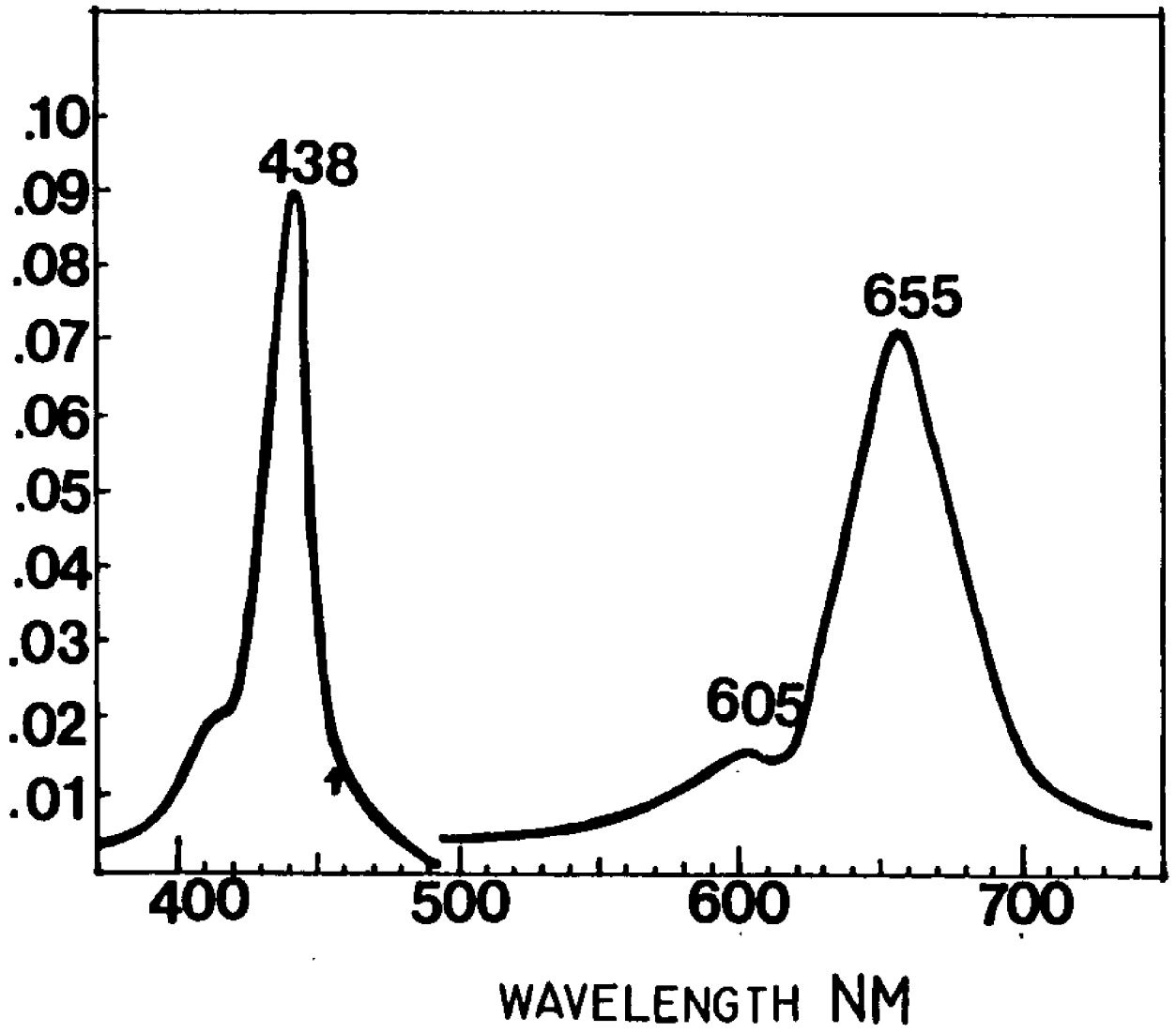
.10
.09
.08
.07
.06
.05
.04
.03
.02
.01
438
655
605
400
500
600
700
WAVELENGTH NM

Figure 10 : Emission spectrum of TPP dissolved in glacial acetic acid at room temperature.

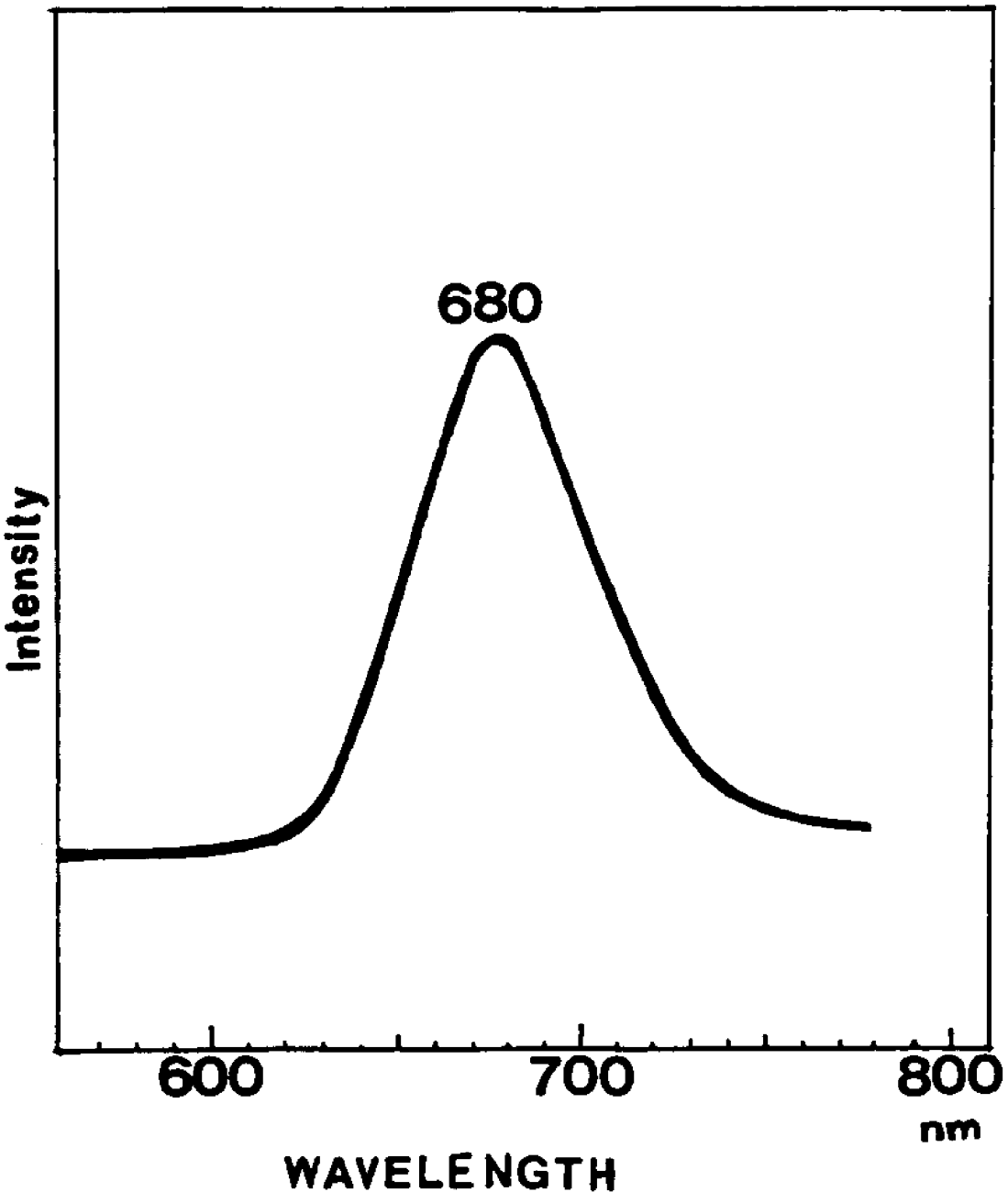
680
Intensity
600
700
800
nm
WAVELENGTH

Figure 11 : Resonance Raman spectra of TPP dissolved in glacial acetic acid. (A) perpendicularly polarized (B) Parallel polarized. Excitation wavelength 457.9 nm. (ca. 50 mW) Approximate spectral slit width 5 cm^{-1}. The spectrum was corrected for luminescence.

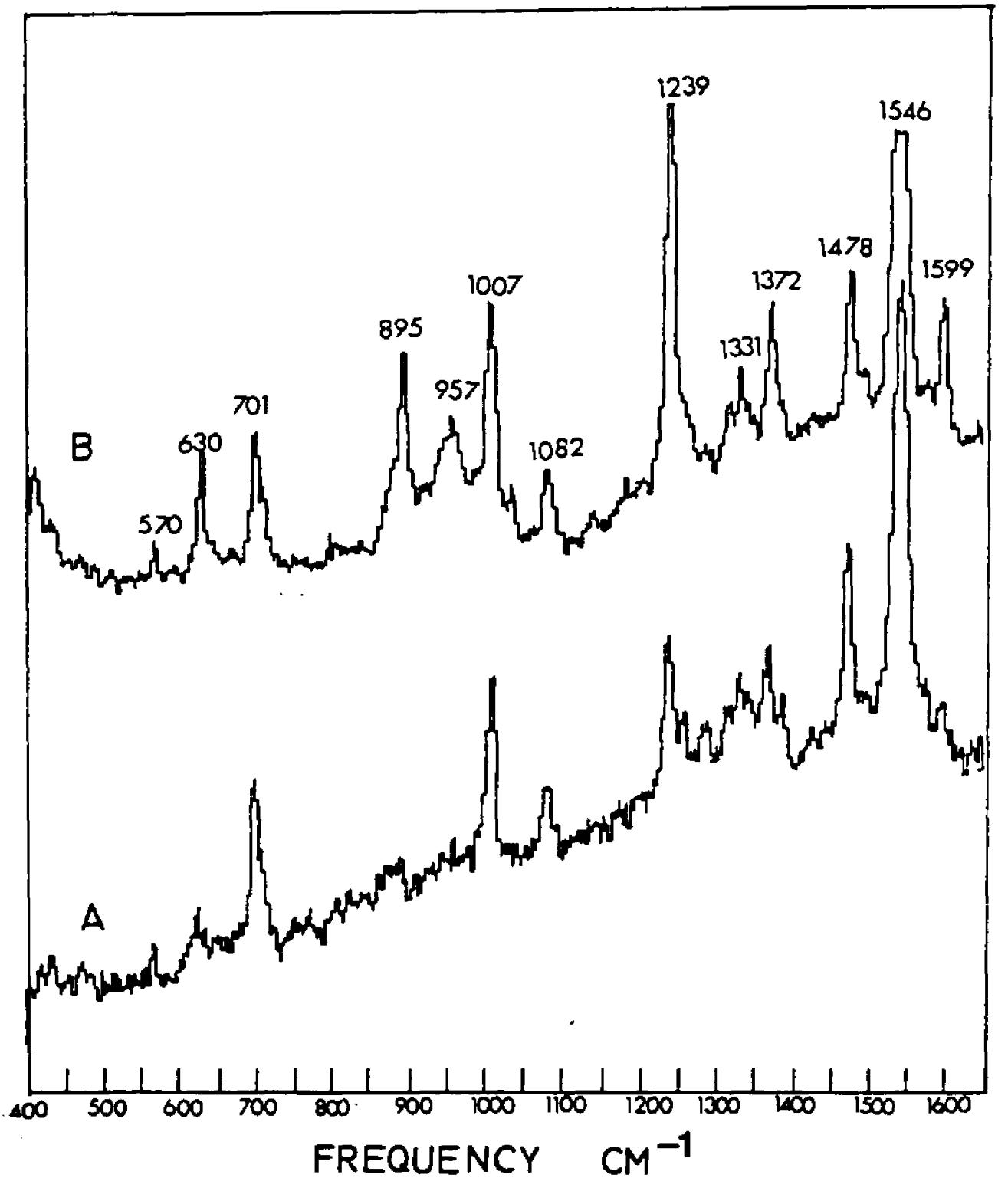
1239
1546
1478
1599
1372
1331
1007
895
957
701
630
570
1082
B
A
400
500
600
700
800
900
1000
1100
1200
1300
1400
1500
1600
FREQUENCY CM⁻¹

Table 13: Comparison of the principal resonance Raman bands (cm^{-1}) of TPP(solid), TPP(adsorbed) and TPP in acetic acid.

Band	TPP(solid)	TPP(adsorbed)	TPP(acid)
1	1600(w)	1601(w)	1599(m)
2	1551(vs)	1546(vs)	1546(vs)
3		1475(w)	1478(m)
4	1440(w)		
5	1380(w)	1385(m)	1372(m)
6			1331(w)
7	1294(m)		
8	1237(s)	1238(s)	1239(s)
9	1080(m)	1085(m)	1082(m)
10	1005(s)	1011(m)	1007(m)
11	966(s)	966(w)	957(w)
12			895(m)
13	839(w)	821(w)	
14		711(m)	701(m)
15	639(m)	635(m)	630(m)

w = weak, m = medium, s = strong, vs = very strong

(b) ZnTPP

Adsorption of ZnTPP onto the PVG surface followed by removal of solvent in vacuo, results in conversion of the red-purple ZnTPP (in solution) to a green material (adsorbate). When the absorption spectrum of ZnTPP adsorbed on PVG (Fig. 13) is compared to the absorption spectrum in methylene chloride solution (Fig. 12) it is clear that ZnTPP has reacted (decrease of 545 nm band) forming product(s) that absorb towards red. Significant initial spectral changes are found within the time required to absorb from solution and pump off the solvent (~30 min), but as shown in Fig. 14, these changes continue for several days. A notable feature of these spectra are bands at about 850 nm and 770 nm which steadily increase with time over several days.

The emission spectrum in solution consist of two bands at 590 and 645 nm, whereas the emission of ZnTPP (adsorbed) consists of a strong emission at 670 nm (Fig. 15). As both TPP (adsorbed) and ZnTPP (adsorbed) emit at approximately the same wavelength it is possible that the species that emits is the same in both instances.

The resonance Raman spectrum, in air, of the ZnTPP on PVG using 457.9 nm laser excitation (Fig. 17) is quite different from the spectrum of solid ZnTPP (Fig. 16). Table 14 provides a comparison of major RR bands. A major difference is the appearance of the most prominent band in the high

frequency region of ZnTPP (solid) at 1552 cm^{-1} and that of ZnTPP (adsorbed) at 1596 cm^{-1}. ZnTPP (solid) shows several strong bands at 1359, 1238 and 1008 cm^{-1} which do not have corresponding bands in the spectrum of ZnTPP (adsorbed). Fig. 18 shows the time dependence of the resonance Raman spectra of ZnTPP adsorbed on PVG. Although significant changes in the absorption were observed during this time period (Fig. 14) no considerable changes in the resonance Raman spectra were noted.

The esr spectrum of ZnTPP adsorbed on PVG was recorded using the same method described earlier for TPP and is given in Fig. 19 The g value calculated is 2.00 and the peak-to-peak first derivative width is 2.55 G. The esr signal in this case is not a smooth curve. The symmetrical pattern on either side of the signal indicates a hyperfine structure. In solution the esr spectrum of ZnTPP cation radical consist of nine lines[22]. The pattern here when closely examined is consistent with nine lines and suggests the presence of ZnTPP cation radical on PVG. The attempts made to enhance the hyperfine structure of the signal were not successful. At liquid nitrogen temperature the hyperfine structure was lost (Fig. 20) due to fast relaxation of the radical. The esr signal disappears immediately when air is introduced to the sample, but can be regenerated by evacuating the sample for several minutes. This cycle was repeated several times with some loss of the signal intensity.

Figure 12: Absorption spectrum of ZnTPP in methylene chloride solution (5×10^{-5} M solution, Soret region 1 mm cell, other 10 mm cell) The arrow marks the excitation wavelength used for the resonance Raman spectrum in Figure 16.

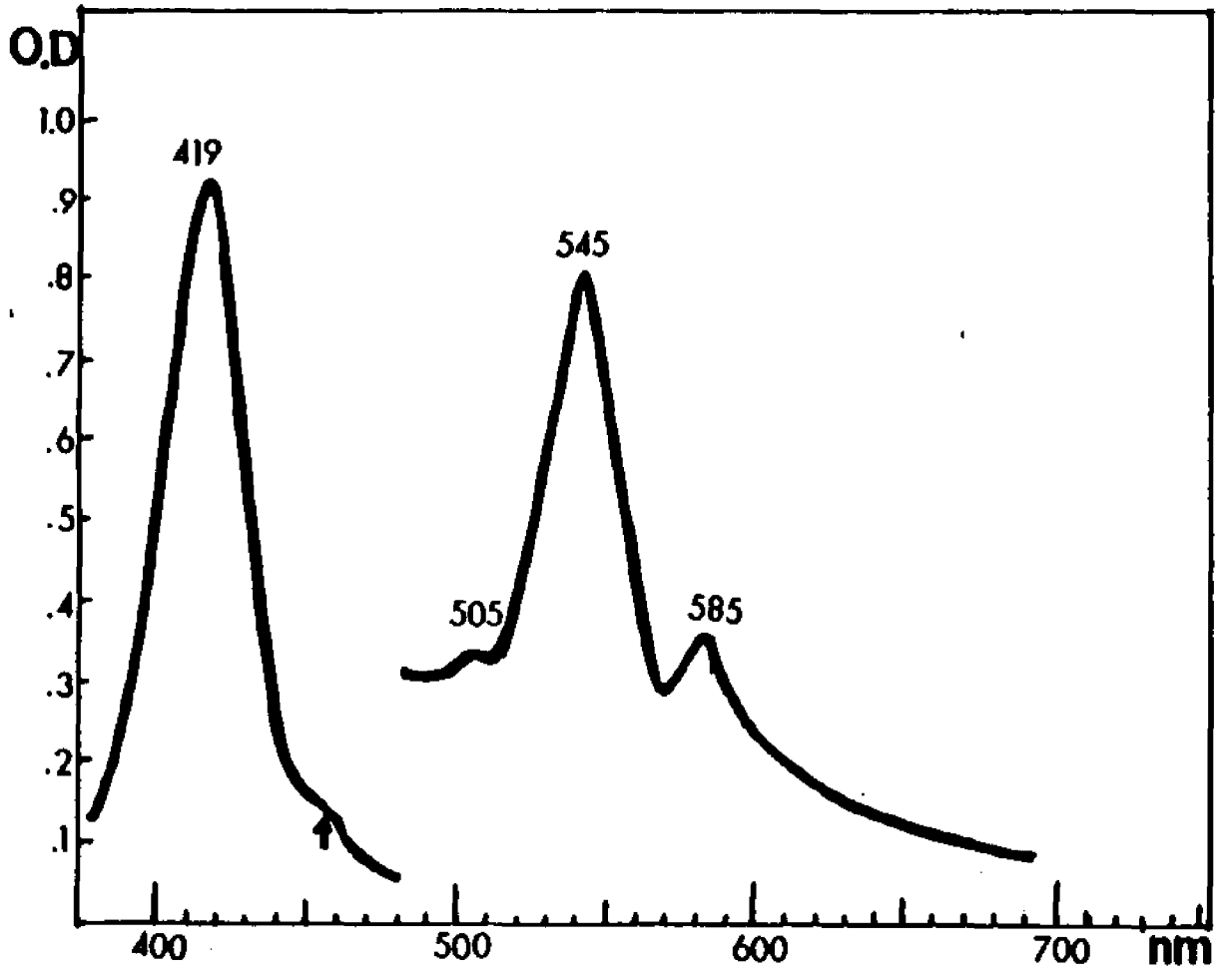

WAVELENGTH

Figure 13 : Absorption spectrum of ZnTPP adsorbed on PVG immediately upon the removal of the solvent. (10^{-6} moles adsorbed on a piece of PVG 25 mm x 25 mm x 4 mm) The arrow marks the excitation wavelength used for the resonance Raman spectrum in Figure 15.

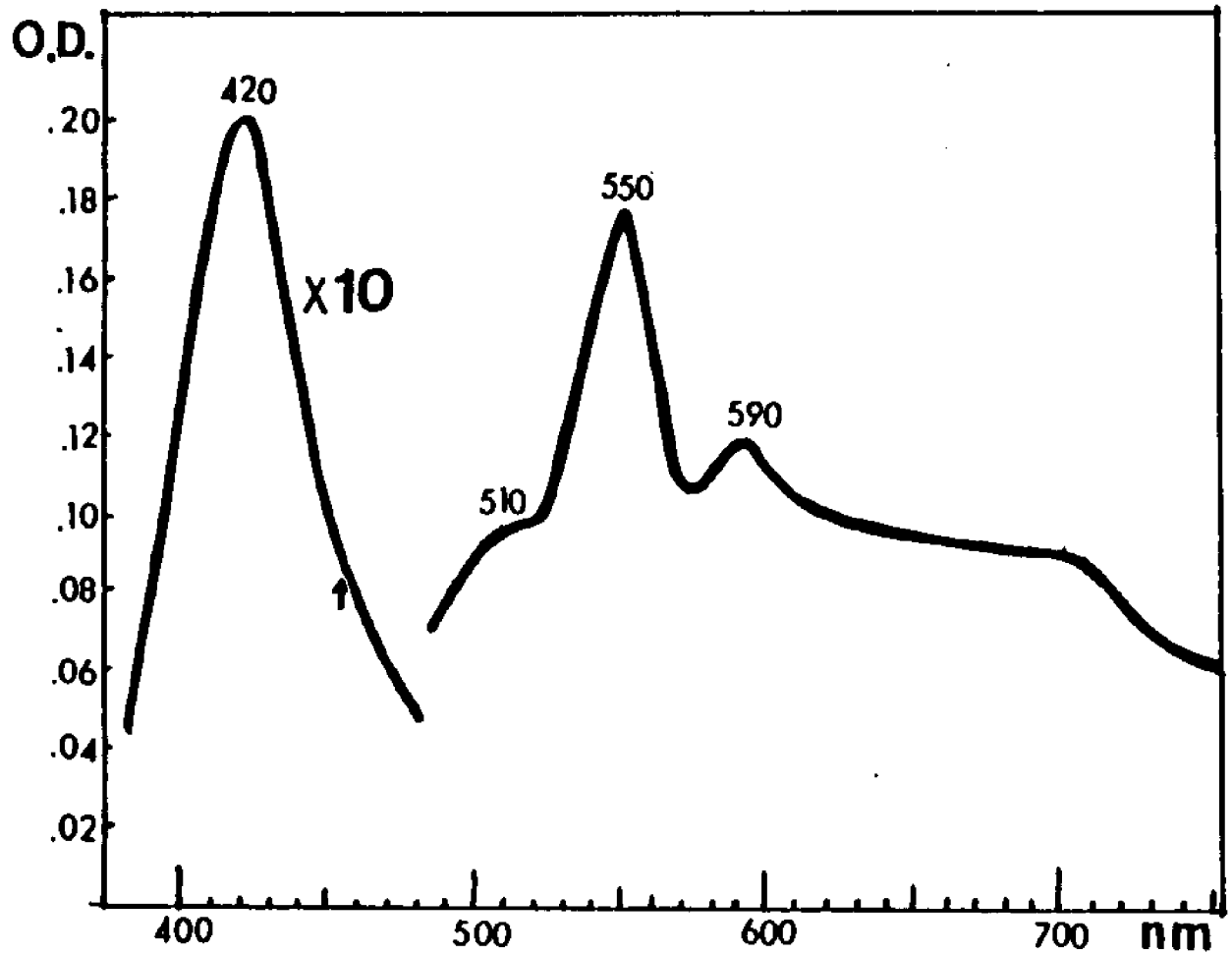
O.D.
.20
.18
.16
.14
.12
.10
.08
.06
.04
.02
420
X10
1
510
550
590
400
500
600
700
nm

WAVELENGTH

Figure 14 : Absorption spectra of ZnTPP in the Visible region (Soret band excluded) at various times after adsorption onto PVG:

(a) Solution spectrum in CH_2Cl_2 (for comparison)

(b) 30 min after adsorption

(c) 2 days after adsorption

(d) 7 days after adsorption

The sample was stored in air.

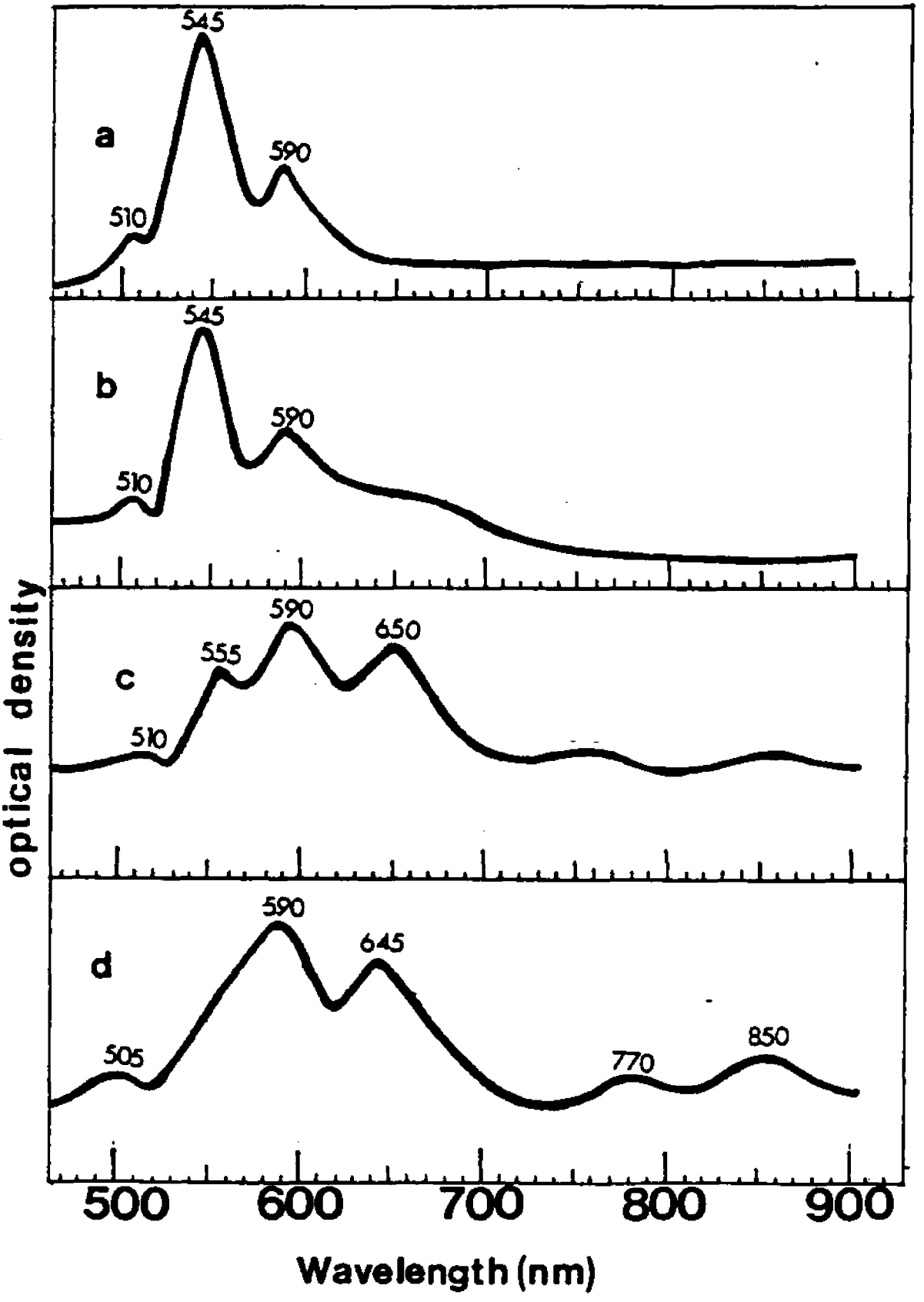
545
a
590
510
545
b
590
510
590
650
555
c
510
590
645
d
505
770
850
optical density
500
600
700
800
900
Wavelength (nm)

Figure 15 : Emission spectra of ZnTPP at 25°C. (a) Adsorbed on PVG (b) In methylene chloride solution.

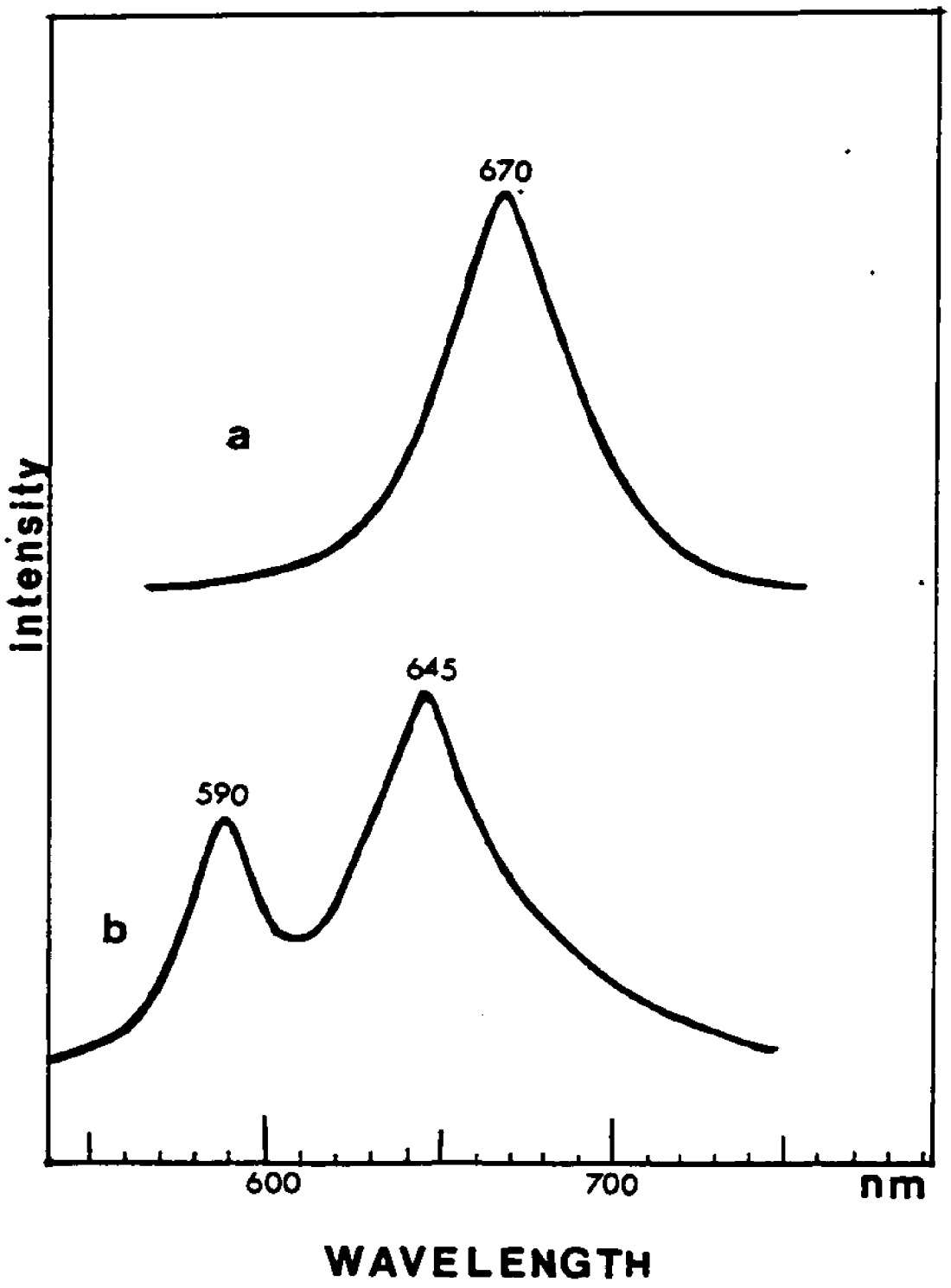
670
a
Intensity
645
590
b
600
700
nm
WAVELENGTH

Figure 16 : Resonance Raman spectrum of solid ZnTPP mixed with KBr at room temperature. Excitation wavelength 457.9 nm (ca. 30 mW). Approximate spectral slit width 5 cm^{-1}. The spectrum was corrected for luminescence.

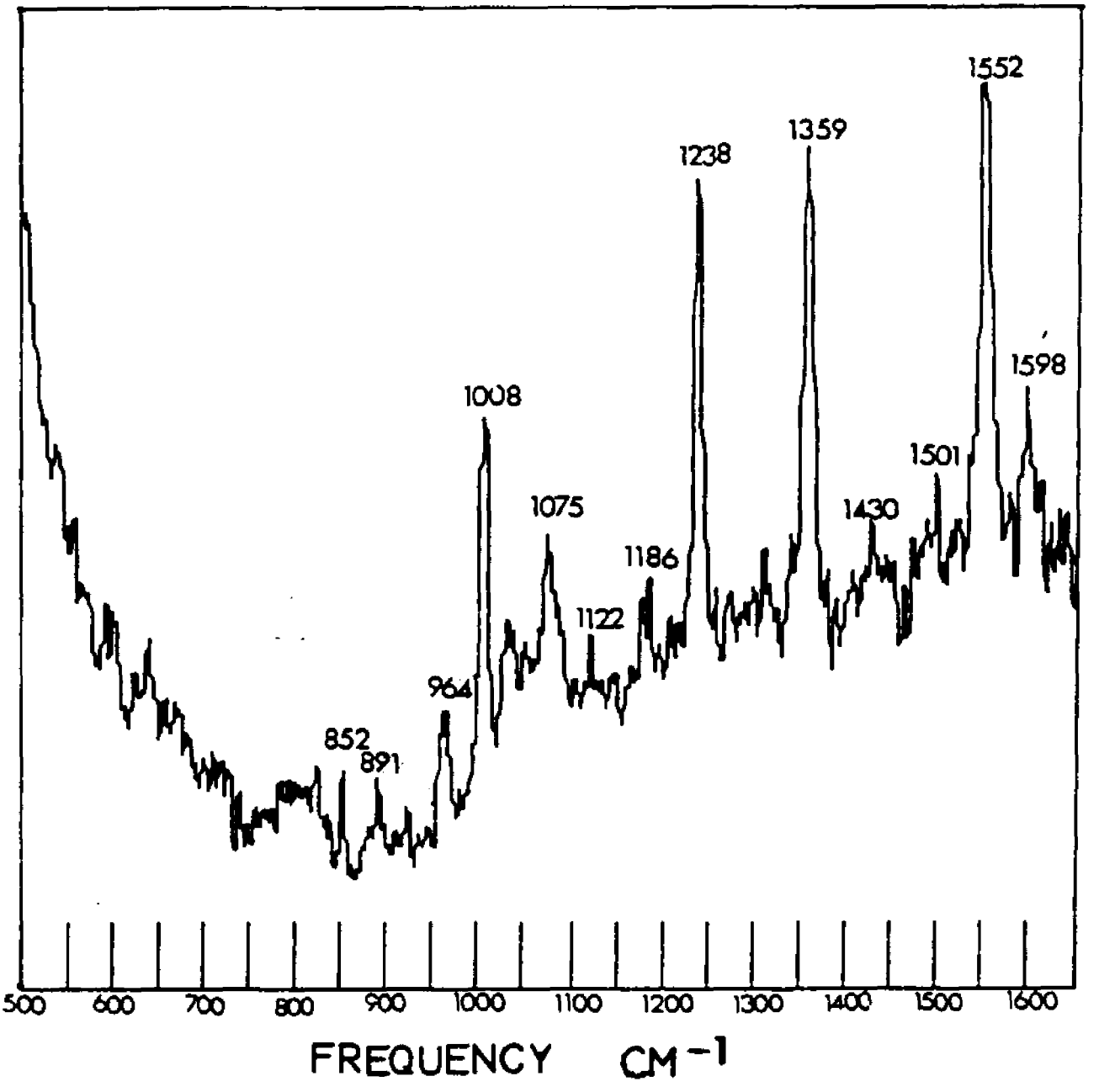
1552
1359
1238
1598
1008
1501
1075
1430
1186
1122
964
852
891
500
600
700
800
900
1000
1100
1200
1300
1400
1500
1600
FREQUENCY CM⁻¹

Figure 17 : Resonance Raman spectrum of ZnTPP adsorbed on PVG 7 days after adsorption. The sample was stored in air. Excitation wavelength 457.9 nm (ca.30 mW) Approximate spectral slit width 5 cm^{-1}. The laser beam was defocussed to avoid sample decay. The spectrum was recorded in air at room temperature and was corrected for luminescence.

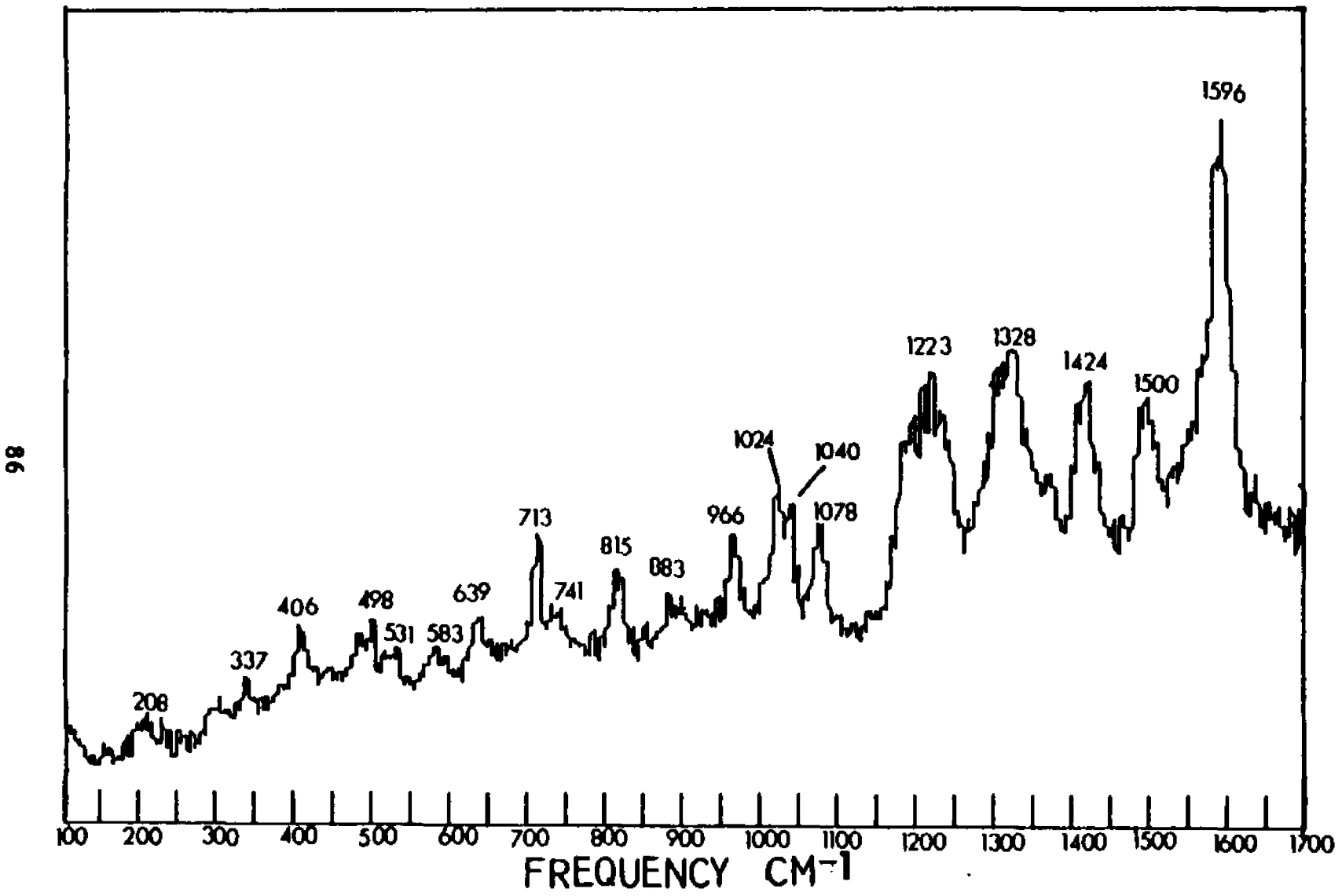
98
208
337
406
498
531
583
639
713
741
815
883
966
1024
1040
1078
1223
1328
1424
1500
1596
100
200
300
400
500
600
700
800
900
1000
1100
1200
1300
1400
1500
1600
1700
FREQUENCY CM⁻¹

Figure 18 : Resonance Raman spectra of ZnTPP at various times after adsorption onto PVG. (A) 30 min (B) 2 days (C) 7 days. Wavelength of excitation 457.9 nm (ca. 30 mW). Approximate spectral slit width 5 cm^{-1}. The laser beam was defocussed to avoid sample decay. The spectra were recorded in air at room temperature and were corrected for luminescence.

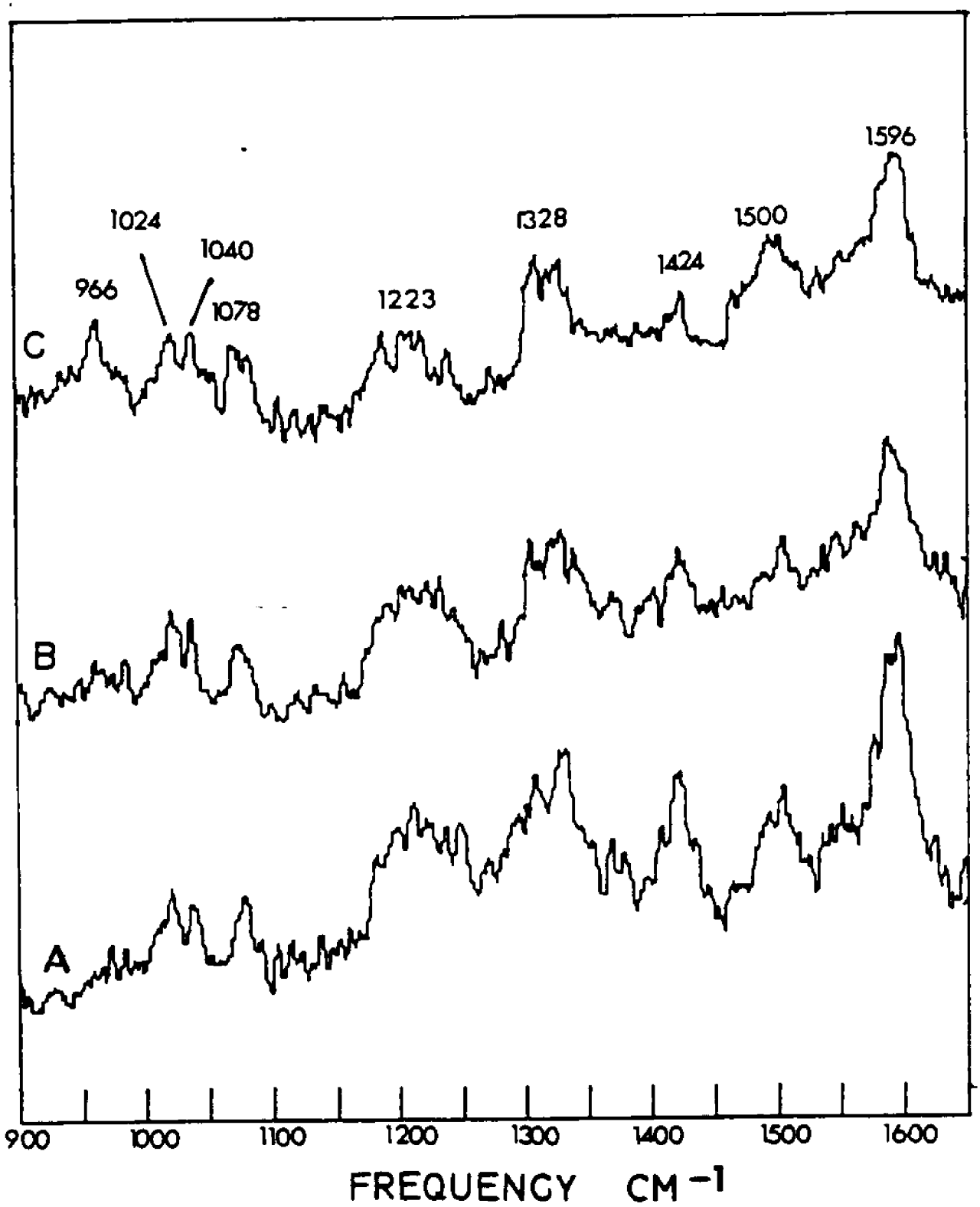
1596
1024
1328
1500
1040
1424
966
1078
1223
C
B
A
900
1000
1100
1200
1300
1400
1500
1600
FREQUENCY CM -1

Figure 19 : Electron paramagnetic resonance spectrum, at 9.78 GHz, of ZnTPP adsorbed onto powdered PVG, then evacuated at 25°C. Spectrum was obtained with 4 mW microwave power using 100kHz modulation (0.25 Gpp) and a gain of 2×10^5.

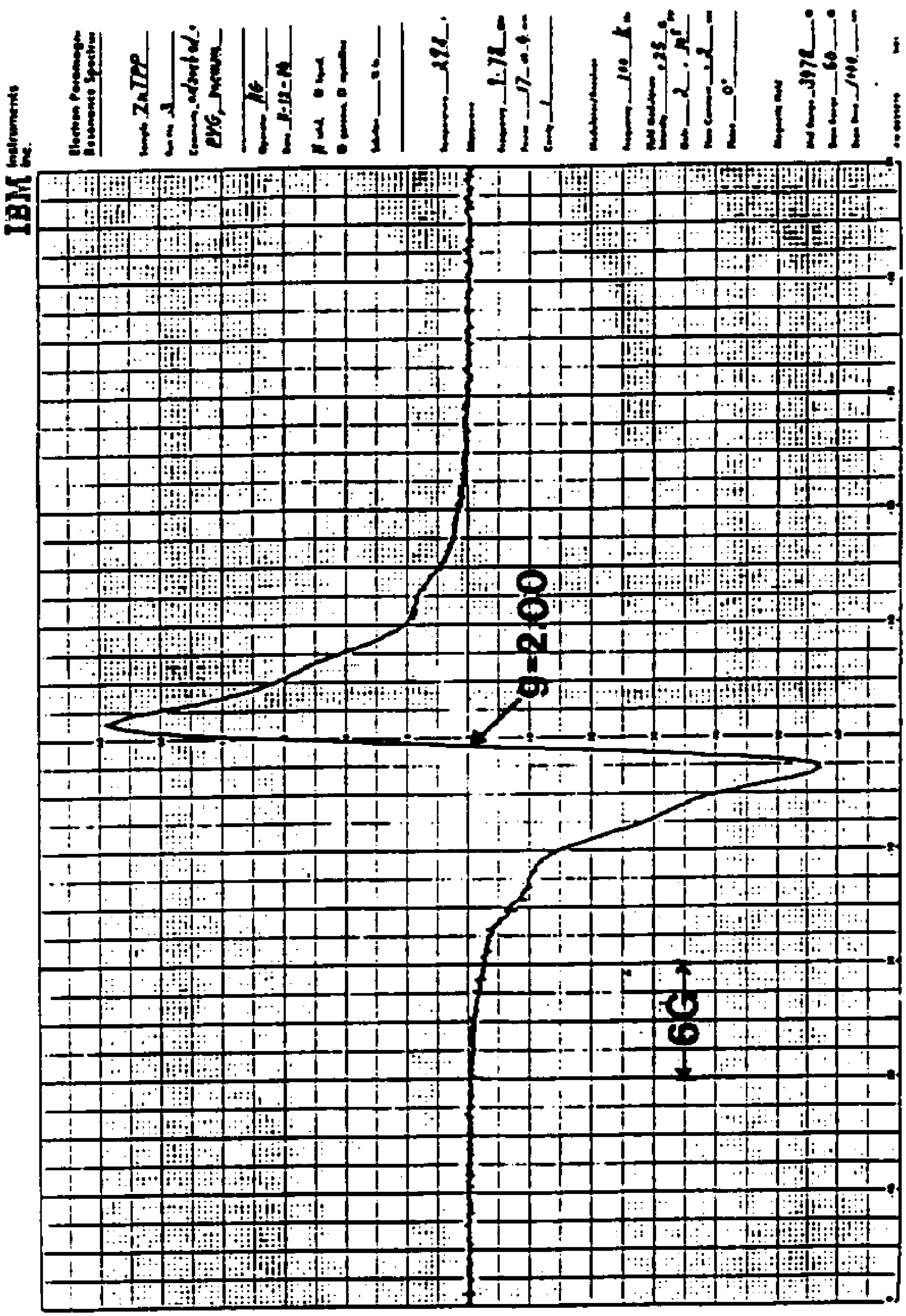
IBM Instruments Inc.
g=2.00
6G

Figure 20 : Electron paramagnetic resonance spectrum, at 9.46 GHz, of ZnTPP adsorbed onto powdered PVG, then evacuated, at 77 K. Spectrum was obtained with 8.1 mW microwave power using 100 kHz modulation (0.25 Gpp) and a gain of 1.25×10^5.

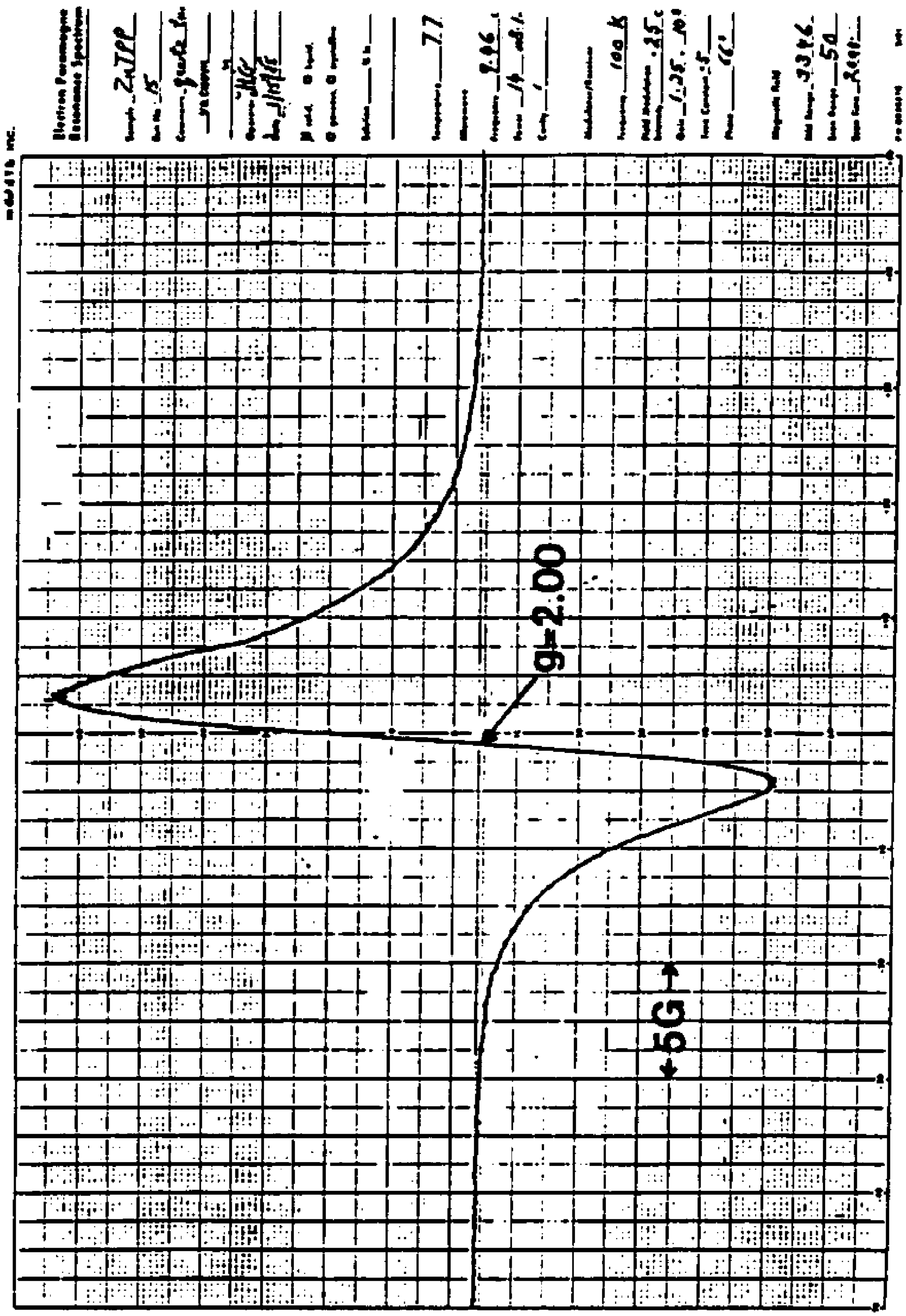
g=2.00
←5G→

Table 14 : Comparison of the principal RR bands (cm^{-1}) of ZnTPP(solid), ZnTPP(adsorbed), MeO-ZnTPP-isoporphyrin (solution) and EtO-ZnTPP-isoporphyrin(solution).

Band	ZnTPP (solid)	ZnTPP (adsorbed)	MeO-ZnTPP isoporphyrin	EtO-ZnTPP isoporphyrin
1	1598(w)	1596(s)	1590(s)	1588(s)
2	1552(s)		1558(vw)	1556(vw)
3			1536(m)	1534(m)
4			1523(w)	1515(w)
5	1501(w)	1500(m)	1497(m)	1489(m)
6			1452(m)	1449(m)
7	1430(w)	1424(m)	1417(s)	1415(s)
8	1359(s)		1368(w)	1366(w)
9		1328(m)	1342(s)	1340(s)
10			1293(s)	1291(s)
11	1238(s)	1223(m)		
12	1186(w)			
13	1122(w)			
14	1075(m)	1078(m)	1079(m)	1077(m)
15		1040(m)	1037(m)	1033(w)
16		1024(m)	1018(s)	1018(s)
17	1008(s)			
18	964(m)	966(m)		
19	891(w)	883(w)		

vw=very weak, w=weak, m=medium, s=strong

(c) Isoporphyrins

Isoporphyrins were prepared starting from ZnTPP using the corresponding alcohol of the nucleophile as the solvent. For example, if methoxy isoporphyrin is to be made, absolute methanol was used as the solvent. For ethoxy isoporphyrin absolute ethanol was used. ZnTPP is only slightly soluble in either of these alcohols. However, enough material goes into solution to give a red-purple colored solution. To this solution a very small amount of solid ceric ammonium nitrate is added. After about 30 seconds, when ceric salt starts to dissolve and react, a deep green color appears. This green color lasts for a minute or so and then turns to a light green color which is permanent. The appearance of deep green color probably corresponds to the initial oxidation of ZnTPP to the cation radical. The light green color corresponds to the formation of isoporphyrin. The absorption spectra of isoporphyrins (Fig. 21 and 22) are very much different from the absorption spectra of most of the porphyrins in that they have absorption bands at 770 and 840 nm. The Soret band too is red shifted and appears at 440 nm.

The resonance Raman spectra of isoporphyrins (Fig. 23) are expected to be strongly resonance enhanced with 457.9 nm excitation because the wavelength of excitation falls within the Soret band. Apart from minor differences the resonance Raman spectra of methoxy and ethoxy isoporphyrins

are similar. There are many bands in the 900-1600 cm^{-1} range that are not present in the RR spectrum of ZnTPP. Table 14 provides a comparison of major RR bands seen in ZnTPP(solid), ZnTPP(adsorbed), Methoxy-ZnTPP-isoporphyrin (solution) and Ethoxy-ZnTPP-isoporphyrin(solution) It is evident that most of the strong and medium bands in ZnTPP(adsorbed) spectrum including the bands at 1596 cm^{-1} agree with the bands in the RR spectrum of isoporphyrins.

For the purpose of verification that these bands are indeed from the isoporphyrin and not from the alcohol or its oxidation products, a resonance Raman spectrum of absolute ethanol with the same concentration of cerric ammonium nitrate used in the preparation of isoporphyrins, was recorded (Fig. 24). The Raman bands observed were quite different from the bands in the isoporhyrin spectrum.

Figure 21 : Absorption spectrum of MeO-ZnTPP-isoporphyrin in methanol solution, ~~solution~~. (6.75×10^{-4} M solution) The arrow marks the excitation wavelength used for the resonance Raman spectrum in Figure 23.

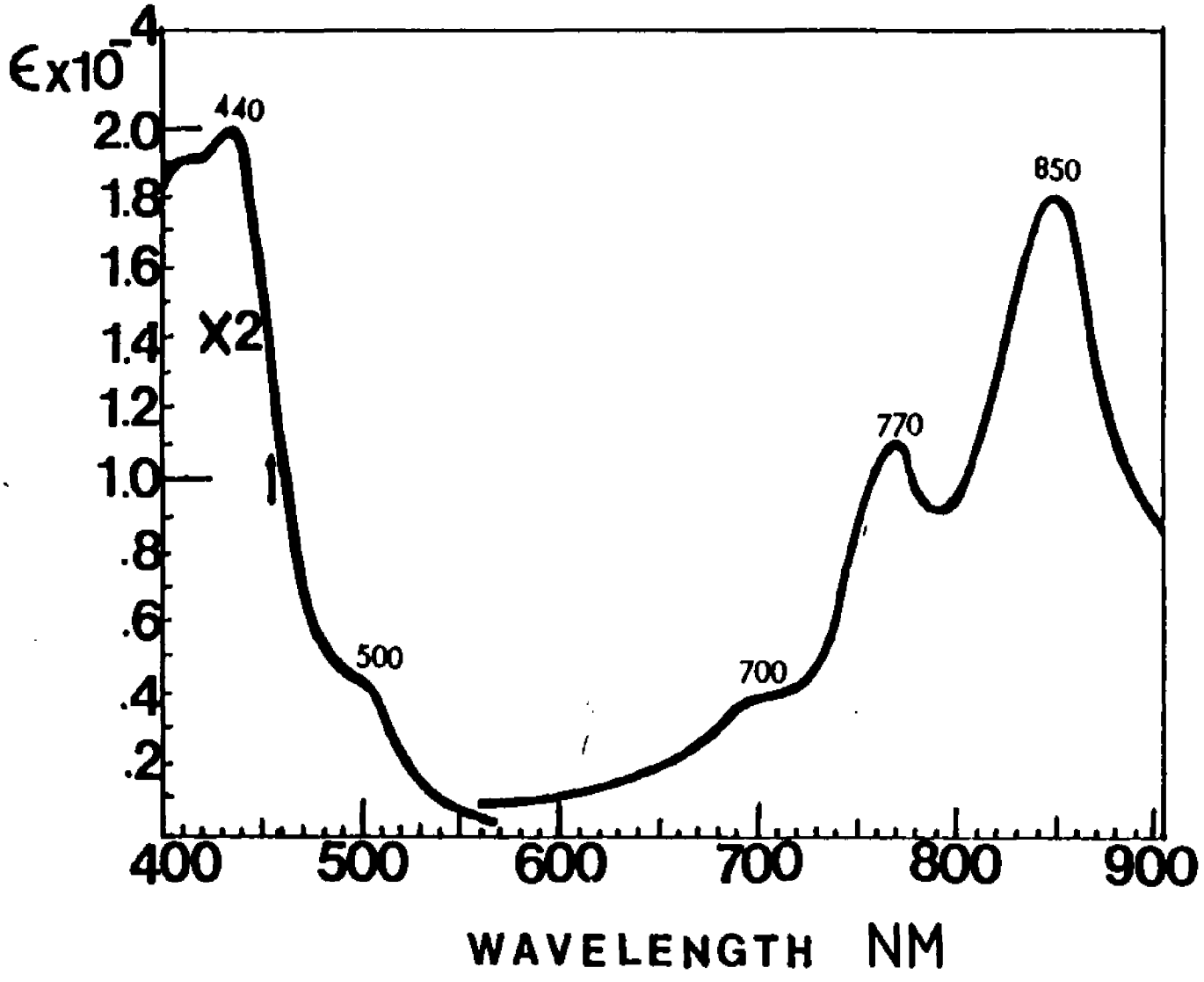
Ex10⁻⁴
2.0
1.8
1.6
1.4
1.2
1.0
.8
.6
.4
.2
X2
440
500
700
770
850
400
500
600
700
800
900
WAVELENGTH NM

Figure 22 : Absorption spectrum of EtO-ZnTPP-isoporphyrin in ethanol solution. (6.4 x 10^{-4} M solution) The arrow marks the excitation wavelength used for the resonance Raman spectrum in Figure 23.

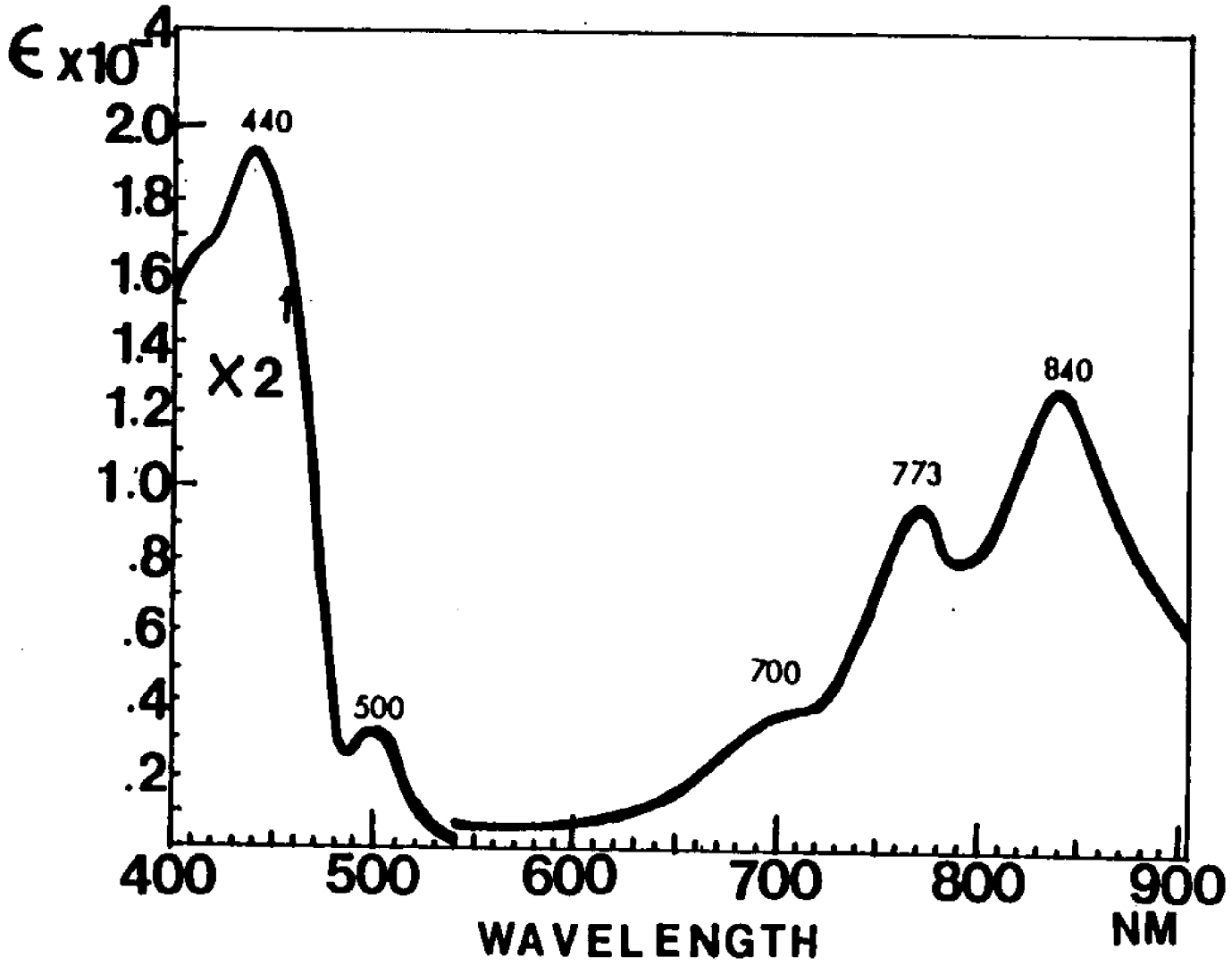
ε x10⁻⁴
2.0
1.8
1.6
1.4
1.2
1.0
.8
.6
.4
.2
440
X2
500
700
773
840
400
500
600
700
800
900
WAVELENGTH
NM

Figure 23 : Resonance Raman spectra of isoporphyrins.
(A) Methoxy-ZnTPP-isoporphyrin in methanol solution
(B) Ethoxy-ZnTPP-isoporphyrin in ethanol solution
Excitation wavelength 457.9 nm (ca. 50 mW). Approximate spectral slit width 5 cm^{-1}. Both spectra were corrected for luminescence.

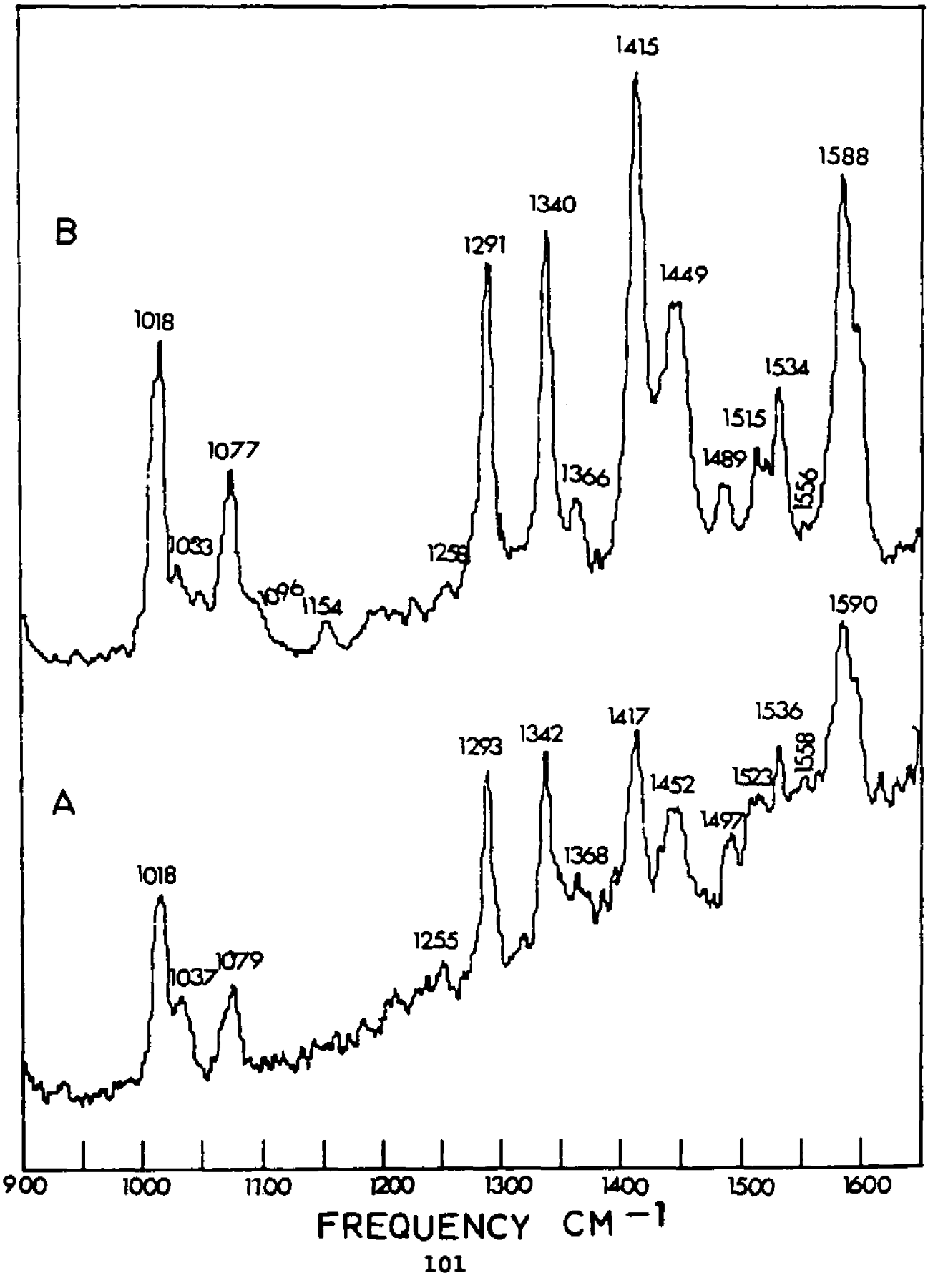
B
1415
1588
1340
1291
1449
1018
1534
1515
1077
1489
1366
1556
1033
1258
1096
1154
A
1590
1536
1417
1293
1342
1558
1523
1452
1497
1368
1018
1255
1037
1079
900
1000
1100
1200
1300
1400
1500
1600
FREQUENCY CM⁻¹

Figure 24 : Raman spectrum of ethanol mixed with ceric ammonium nitrate. Wavelength of excitation 457.9 nm (ca. 100 mW) Approximate spectral slit width 5 cm^{-1}.

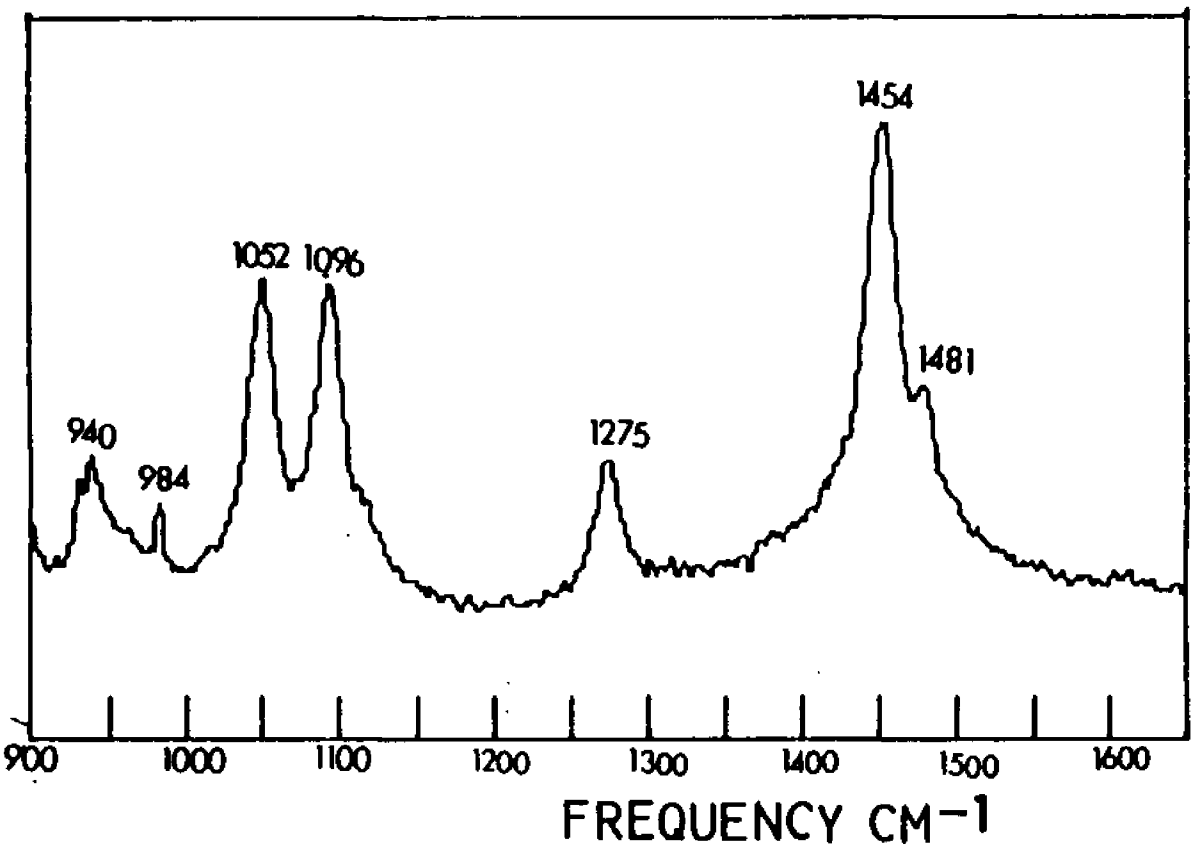
1454
1052
1096
1481
940
984
1275
900
1000
1100
1200
1300
1400
1500
1600
FREQUENCY CM-1

(C) CONTROL EXPERIMENTS IN OXYGEN FREE ATMOSPHERE

The sample of PVG made by adsorbing porphyrins in an oxygen free atmosphere did not show any green color or an epr signal as long as it was allowed remain under vacuum. When exposed to air the epr signal slowly increased and after about 12 h a signal equal in intensity to a signal of a sample which was not degassed was obtained. The color of the sample gradually turned green. However if the sample of PVG heated to less than 60^{o}C in the vacuum certain amount of green color appeared with an associated weak epr signal.

The Absorption spectra recorded in oxygen free atmosphere showed only the initial changes depicted in fig. 14-b. If stored in oxygen free atmosphere the growth of bands at 770 and 850 nm was not observed for a period of three weeks. A similar situation was observed with resonance Raman spectra. If the samples were stored in oxygen free atmosphere in an epr tube the Raman bands observed were mainly those of ZnTPP(solid).

(D) DECARBONYLATION REACTIONS

Decarbonylation reactions were carried out a number of times, but did not proceed catalytically. When mixed with reactants in the reaction mixture benzene (the product expected from benzaldehyde) and toluene (the product expected from phenylacetaldehyde) yielded a significant response on gas chromatograph in mmol quantities. However, these hydrocarbons were never observed in the reaction mixture as products. Minor modifications of the procedure and purification of solvents by distillation prior to use failed to produce any results. It was evident, however, that bis-phosphine $RuTPP(PPh_3)_2$ is converted to the mono-phosphine $RuTPP(PPh_3)CO$ in the presence of CO gas or aldehyde. Mono-phosphine compound was found to be unstable, forming RuTPPCO on standing and on dilution. The absorption spectra of these species are illustrated in Fig 25

$RuTPP(PBu_3^n)_2$ is easily formed on addition of stoichiometric amounts of PBu_3^n to RuTPPCO. The absorption spectrum of this species (Fig 26) did not change upon addition of aldehyde or passage of CO, which demonstrated the stability of this species.

Figure 25 : Absorption spectra of $RuTPP(PPh_3)_2$ (—●—) and $RuTPP(PPh_3)CO$ (——) in benzene.

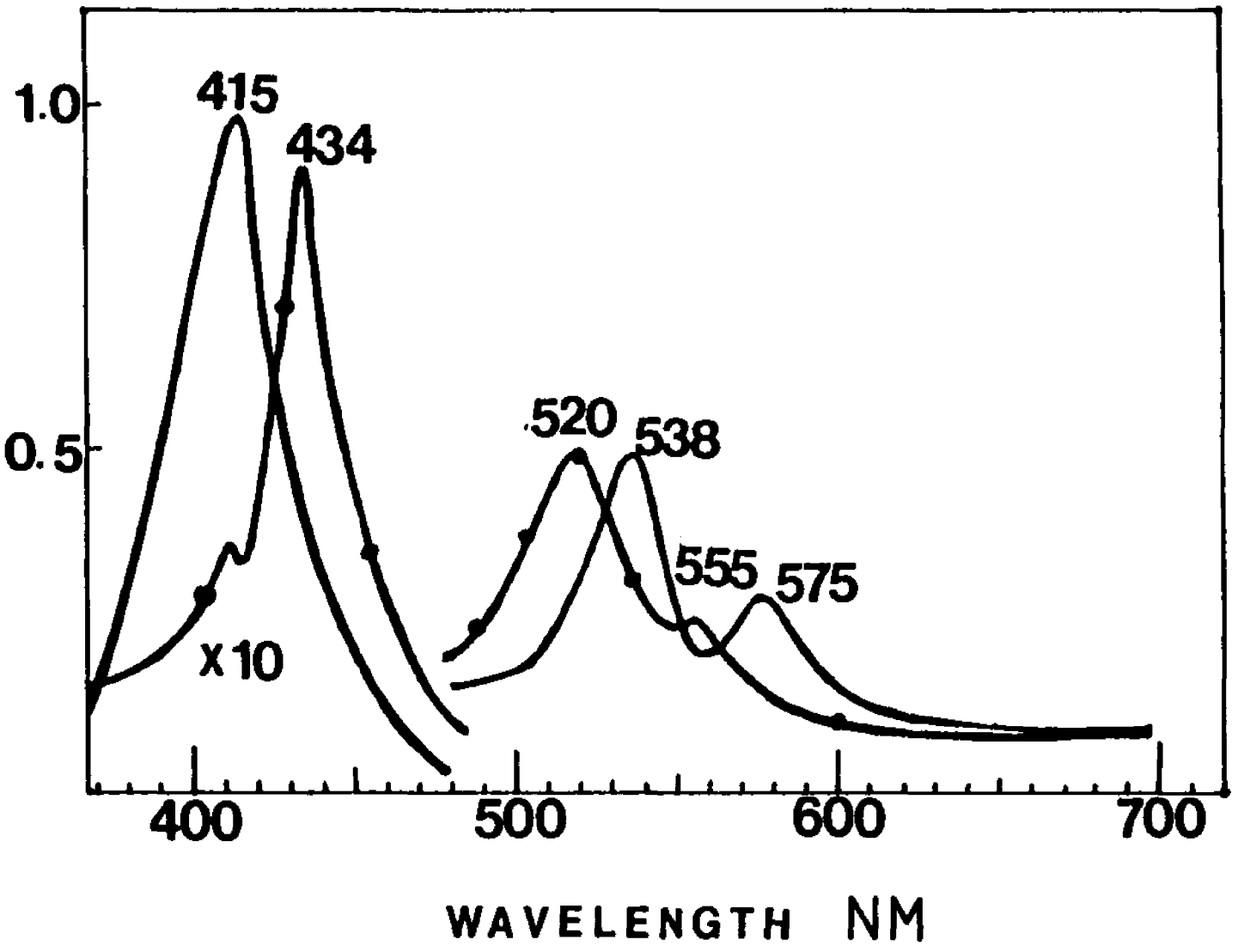
1.0
0.5
415
434
520
538
555
575
X 10
400
500
600
700
WAVELENGTH NM

Figure 26 : Absorption spectra of $RuTPP(PBu^n_3)_2$ (—•—) and RuTPPCO (——) in methylene chloride.

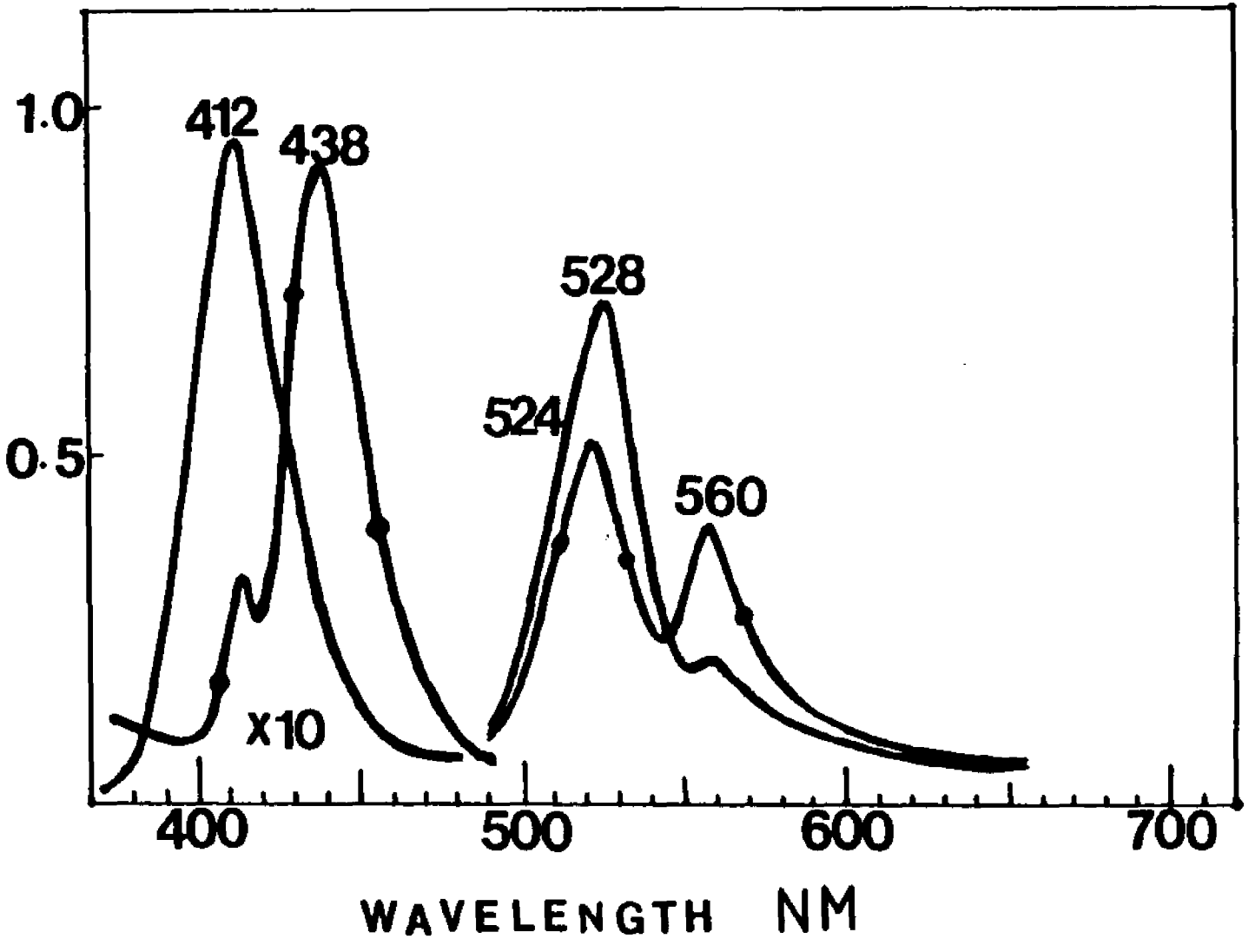
1.0
0.5
412
438
528
524
560
x10
400
500
600
700
WAVELENGTH NM

4. DISCUSSION

(a) Surface acidity of PVG

The ratios of optical densities given in tables 11 and 12 can be used to obtain an approximate value for the surface pH of PVG. With cresol red indicator for buffer solutions having pH values greater than 3.0 the absorption maximum at 520 nm is absent. For PVG a strong absorption band at 432 nm was obtained but none at 520 nm. Therefore based on these results it is reasonable to assume that the surface pH of PVG is more than 3.0. With bromocresol green buffer solutions having pH values less than 4.0 did not show any absorption at 615 nm. PVG with the same indicator did not show any absorption at 615 nm even though it showed some absorption at 440 nm. Therefore using these two indicators we are able to set approximate upper and lower limit values for the surface pH of the PVG sample, 4 and 3 respectively. It should be mentioned, however, that different samples of PVG tend to have slightly different surface acidities. Such variations are not very significant and it was found that most of the samples used in our study have pH values within the above mentioned range. The surface acidity of PVG plays an important role in its surface chemistry.

(b) TPP

The absorption spectrum of TPP changes when adsorbed onto PVG (Figs. 3 and 4). Appearance of a Soret band at 450 nm clearly indicates the formation of a different compound. The intensity pattern of the four bands in the visible region of the spectrum of TPP in solution has been changed. This change can be associated with a strong absorption maximum at 660 nm of the second species with a Soret band at 450 nm. The solution absorption spectrum of H_4TPP^{2+} consists of a Soret band at 445 nm, a strong band at 661 nm and a weak band at 608 nm[89]. Therefore the absorption spectral evidence indicates that the TPP undergoes protonation on the surface of PVG to form the diacid. The protons are provided by the silanol groups of the surface. The emission spectra provide further proof of this fact. The emission maximum at 680 nm (fig. 5) of TPP adsorbed on PVG corresponds to the emission maximum observed of TPP in glacial acetic acid (fig. 10). Although the absorption spectrum (fig. 4) indicates that there is unprotonated TPP on the surface of PVG, the strong emission from the protonated TPP completely masks the emission from the free base.

The formation of the diprotonated TPP on the surface of PVG can be explained using the pK values of H_2TPP given earlier (page 11). The values of 4.4 and 3.9 have been observed for pK_3 and pK_4 respectively[12]. According to the

scheme introduced by Phillips[91] the pK_3 and pK_4 are defined as:

$$pK_3 = pH - \log [PH_2]/[PH_3^+]$$

$$pK_4 = pH - \log [PH_3^+]/[PH_4^{2+}]$$

Therefore if present in a medium of pH 3 (which is the measured lower limit of surface pH of PVG) the following calculation shows that H_2TPP should be readily protonated to the mono and dications, at equilibrium.

From the equation (1) above using the values of $pK_3 = 4.4$ and pH = 3

$$\log [PH_2]/[PH_3^+] = -1.4.$$

Therefore at equilibrium, the concentration of PH_3^+ could be as much as 39.8 times the concentration of PH_2. Similar calculation using the equation (2) will show that the concentration of PH_4^{2+} could be upto 7.9 times that of PH_3. For PVG samples with slightly higher surface pH values the extent of protonation could be less.

The resonance Raman spectra provide further evidence of this reaction (table 13). The TPP (adsorbed) spectrum contains bands common to both TPP (solid) and TPP(acid). Especially the band at 1475 cm^{-1} has a corresponding band in TPP (acid) but not in TPP (solid). Similarly the band at 711 cm^{-1} has a corresponding band in TPP (acid). This shows the presence of TPP and H_4TPP^{2+} on PVG.

The esr signal of TPP on PVG (fig. 8) indicates the formation of a radical on the surface. The porphyrins and metalloporphyrins are known to produce stable cation radicals by anodic oxidation in the presence of an appropriate electrolyte or by chemical oxidation. However, there has not been any report of formation of cation radicals of metalloporphyrins merely by depositing on a support. Many molecules containing π-electrons and heteroatoms with unshared pairs are known to be oxidized to cation radicals when deposited on acidic surfaces[25]. As the surface of PVG is acidic and porphyrins belong to the above mentioned group of molecules it can be stated with certainty that TPP undergoes oxidation to produce π-cation radicals when adsorbed on PVG. The esr signal observed is weak even at a gain of 10^6 with 20 mW power. A strong esr signal was observed for ZnTPP at a low gain. This indicates that TPP undergoes oxidation only to a lesser extent on PVG than ZnTPP. This could be mainly due to the higher first oxidation potential of TPP (0.95 Volts) compared to ZnTPP (0.71 Volts) (table 3).

(c) ZnTPP

The absorption spectral changes observed when ZnTPP is adsorbed on PVG are dramatic. Immediately upon removal of the solvent the PVG appears green compared to the red-purple color in solution. The absorption spectrum shows increased absorption in the 600-700 nm region. If this piece of PVG is stored in air the absorption spectrum continue to change (fig. 14). Of particular interest to us was the appearence of the absorption maxima at 770 nm and 850 nm after about 24 hours which continued to increase over a period of 7 days. Only a few porphyrins and their derivatives show absorption this far towards red. The esr spectrum of ZnTPP adsorbed on PVG indicates (fig. 19) the production of a π-cation radical. For ZnTPP this first ring oxidation occurs at a comparatively low potential ie. 0.71 volts (table 3). The second ring oxidation, removal of an electron from the π-cation radical to produce the dication, also occurs at a fairly low potential ie. 1.03 volts. Therefore if the π-cation radical undergoes oxidation to the strongly electrophilic dication[20], it could react with any nucleophile present on the surface. The silanol groups present on the surface of PVG provide the nucleophilic $Si-O^-$ group. If, as mentioned for methoxy and ethoxy groups, this siloxy group reacts with the dication in the same manner it could form the siloxy-ZnTPP-isoporphyrin on the surface of PVG. These reactions are summarized below:

$$ZnTPP(solution) \longrightarrow ZnTPP(adsorbed) \quad .....(1)$$

$$ZnTPP(adsorbed) - e \longrightarrow ZnTPP^{+\cdot}(adsorbed) \quad .....(2)$$
cation radical

$$ZnTPP^{+\cdot}(adsorbed) - e \longrightarrow ZnTPP^{2+}(adsorbed) \quad .....(3)$$
cation radical dication

$$ZnTPP^{2+}(adsorbed) + Si\text{-}O^{-} \longrightarrow (Si\text{-}O\text{-}ZnTPP\text{-}isoporphyrin)^{+} \quad .....(4)$$
dication PVG surface

The comparison of the absorption maxima seen at 770 nm and 840 nm with the published spectra of isoporphyrins[20,32] shows that these bands are due to the isoporphyrins formed on the surface of PVG. The reactions (3) and (4) take place slowly on PVG. As indicated in the absorption spectra, we do not see any absorption in 700-900 nm region within the first 24 hours of adsorption. The bands at 510, 545 and 590 nm are due to the unchanged ZnTPP. These bands too continue to change with time. In the final spectrum there are bands at 505, 590 and 645 nm. These bands ,which are not due to the isoporphyrin could be due to other oxidation products of the π-ring or demetallated, diprotonated species. However, the product(s) that absorb at 505, 590 and 645 nm seem to be stable, as no further change in the absorption spectrum was observed even after 30 days.

The resonance Raman spectra provide further proof of the formation of isoporphyrins on the surface of PVG. The

wavelength of excitation used in all of our Raman spectra was 457.9 nm line which is the line closest to the UV available on Ar^+ ion laser. Although fairly good resonance enhancement was seen for TPP which has the Soret band at 416 nm in solution, when adsorbed on PVG greater enhancement of the bands due to H_4TPP^{2+} is observed since it has the Sore t

band at 450 nm. A similar situation occurs in the case of ZnTPP. The Soret band of ZnTPP occurs at 419 nm (fig. 12). The isoporphyrins have their Soret bands at 450 nm. Therefore the bands due to isoporphyrins are expected to be highly resonance enhanced with 457.9 nm excitation. The comparison of RR spectra of ZnTPP (solid) with ZnTPP (adsorbed) (table 14) reveals the presence of the bands due to isoporphyrins on PVG when compared to bands due to methoxy and ethoxy isoporphyrins. The band at 1596 cm^{-1} which is the strongest band in the adsorbed spectrum corresponds to the 1590 cm^{-1} band of methoxy and 1588cm^{-1} band of ethoxy isoporphyrins shifted up from the 1552 cm^{-1} band seen for ZnTPP (solid). This band is almost certainly due to the siloxy-isoporphyrin present on PVG.

The assignment of Raman bands to porphyrin vibrational modes is usually on the basis of polarization and deuterium shift measurements. When adsorbed on PVG the movement of the porphyrin molecule as a whole is severely restricted. Therefore the polarization spectra will not be useful. The assignment of bands to several resonance enhanced phenyl modes in RR spectra of $(FeTPP)_2O$[38] and MgTPP, ZnTPP and

CuTPP and their π-cation radicals[42] can be used here. There are major differences in the spectra of TPP(solid) and TPP(adsorbed) from metalloporphyrin spectra. The bands associated with phenyl ring at 1600, 1030, 995 and 890 cm^{-1}, [38] are either absent (890 cm^{-1}) or shifted (1080 and 1005 cm^{-1}) in TPP. A comparison of the bands observed in RR spectra of ZnTPP (table 14) with the reported assignments is given in table 15.

The assignments made in table 15 help to assign the 1596 cm^{-1} band of ZnTPP(adsorbed) to the same mode as 1552 cm^{-1} band of ZnTPP (solid), a ring stretch coupled with a C-H wag. This represents an increase in frequency of 40 wavenumbers when the isoporphyrin is formed. Similarly the band at 1328 cm^{-1} of ZnTPP(adsorbed) can be assigned to correspond to the band at 1359 cm^{-1} of ZnTPP(solid). This represents a decrease of 31 wavenumbers. As the vibration at 1552 cm^{-1} refers to the C_β-C_β stretch and the vibration at 1359 cm^{-1} refers to the C_α-N stretch these assignments mean that when the isoporphyrin is formed the C_β-C_β bond is strengthened and C_α-N bond is weakened.

Table 15: Comparison of the assigned RR bands of ZnTPP (solution) with the observed RR bands of ZnTPP (solid) and ZnTPP (adsorbed).

ZnTPP[a] (solution)	ZnTPP (solid)	ZnTPP (adsorbed)	assignment
		1596	
1550	1552		$\nu(C_\beta - C_\beta) + \delta(C_\beta - H)$
1490	1501	1500	$\nu(C_\beta - C_\beta)$ (B_{1g})
1354	1359		$\nu(C_\alpha - N) + \delta(C_\beta - H)$
		1328	
1235	1238	1223	$\nu(C_m - C_\phi)$
1068	1075	1078	$\delta(C_\beta - H)$
1004	1008		phenyl, $\nu(C_\alpha - C_m)$
882	891	883	phenyl

a) from ref. 42.

The other interesting feature is the absence of the 1008 cm^{-1} band due to phenyl mode in the spectrum of ZnTPP(adsorbed). A similar situation was observed with RR spectra of TPP. In the RR spectrum of TPP(solid) a sharp band at 1005 cm^{-1} was observed, but in the spectrum of TPP(adsorbed) this band is absent. As the 1008 cm^{-1} band of ZnTPP(solid) and 1005 cm^{-1} band of TPP(solid) are both due to the phenyl modes it may be possible that these bands are not resonance enhanced when the compound is adsorbed on PVG. The appearence of Raman bands assignable to the internal modes of the phenyl rings, in resonance with the porphyrin $\pi - \pi^*$ transition, demonstrates the interaction between the phenyl and porphyrin π-systems. In the ground state the phenyl rings are known to be tilted by angles from 21 to 90° and there is substantial barrier to rotation. π-overlap in the ground state is therefore expected to be slight[38]. Resonant enhancement of Raman intensities depends on Frank-Condon or Vibronic factors in the resonant excited state. Consequently, phenyl interaction in the excited state is sufficient to account for the resonance enhancement of the phenyl modes. However, if when adsorbed on PVG, there is a considerable interaction of phenyl groups with the porphyrin π-system in the ground state the resonance enhancement of the phenyl modes may be either reduced or completely absent.

The emission spectrum of ZnTPP adsorbed on PVG cannot be explained on the basis of formation of isoporphyrins (fig

15). The isoporphyrins do not emit at this wavelength. The similarity to the emission spectrum of TPP adsorbed on PVG (fig 5) suggests that here too the emitting species is the diprotonated H_4TPP^{2+}. It is possible that some ZnTPP undergoes demetalation when adsorbed on PVG, and subsequent diprotonation.

The resonance Raman spectra recorded of the same piece of PVG with adsorbed ZnTPP at different time intervals (fig 18) did not reflect all the changes observed in the absorption spectra. The ratio of intensities of the bands remained the same. No increase in the 1596 cm^{-1} band with respect to the other bands was observed. It is possible that some isoporphyrins are formed immediately after adsorption of ZnTPP on PVG, although not detectable in the absorption spectra. Because of the Soret at 450 nm, it would be strongly resonance enhanced with 457.9 nm excitation. The difficulty of mounting the PVG in the Raman spectrometer and aligning the laser beam such that the same spot of the PVG is examined every time a spectrum is recorded, may also have contributed to the nature of the results obtained. The broad nature of the bands also may mask any changes in the intensity.

The hyperfine structure of the $ZnTPP^+$ ClO_4 cation radical esr specrum shows nine lines due to the coupling of four N (I=1) atoms[22]. The calculated ratio of intensity of these nine lines is 1:4:10:16:19:16:10:4:1. These lines

could be further split by the eight equivalent hydrogens at β positions. In solution a_N=1.58 G and a_H=0.316 G. The computed width of the signal (between the two smallest peaks) is therefore 1.58 X 8 = 12.64 G. The width of the signal on PVG is much broader and the smallest peaks are not clearly visible. It is not surprising that the two smallest peaks, which are expected to have only 1/19 th of the height of the largest peaks, cannot be clearly seen. However, their positions can be estimated in comparison to the positions of the other peaks. The splittings due to protons cannot be resolved. The measured width of the signal on PVG (estimating the positions of the two smallest peaks) is 24 G and therefore the a_N = 3.0 G.

The positions and splittings of the lines (specified by the g-values and hyperfine constants) depend on the direction of the magnetic field relative to the molecular axes[92]. This type of spectral anisotropy is not seen in solutions, since in these systems the free electron is extensively delocalized and therefore the anisotropy is small, and also because the rapid random motion of the radicals in solution averages out all the remaining anisotropic splittings and shifts. This kind of rapid averaging gives rise to the chracteristically narrow linewidths in which the hyperfine splittings are well resolved. If the random motion of the molecules are severely restricted, as in a solid sample or when adsorbed on a support, the anisotropy of the spectra between the

three principal directions is clearly seen, both in the hyperfine splittings and in the g-value positions about which the lines are centered. Intermediate spectra are obtained for the orientations between the principal directions. The spectral anisotropy is normally completely specified by the three g-values (g_{zz},g_{xx} and g_{yy}) and hyperfine splittings obtained parallel to the principal axes (A_{zz},A_{xx} and A_{yy}). As ZnTPP is axially symmetrical the principal values are designated as $A_{//} = A_{zz}$: $A_{\perp} = A_{xx} = A_{yy}$ and $g_{//} = g_{zz}$: $g_{\perp} = g_{xx} = g_{yy}$. As $A_{//}$ and $A_{\perp}$ can be very different the A value of approximately 3 G observed on PVG, compared to 1.58 G can be attributed to the spectral anisotropy due to the above mentioned reasons. The difference in peak heights from the calculated values is due to the overlap of the peaks which are broader than usual.

It is not clear why the esr signal disappear when air is introduced and reappears when pumped off. Although line broadening due to paramagnetic molecular oxygen is known to broaden the esr signals, it does not make the signal disappear. A possible explanation for this is a chemical interaction of the radical with air thereby reducing the concentration of the radical to a very low level. The low temperature (77 K) spectrum of ZnTPP adsorbed on vacuum did not reveal any additional evidence. The line is slightly broader than the room temperature signal. The hyperfine structure was lost probably due to the fast relaxations.

(d) Control experiments

As the formation of the cation radicals on the surface of the PVG can be inhibited by thorough degassing, there is no doubt that molecular oxygen plays a part in the oxidation of the porphyrins on the surface of PVG. However, if PVG is not heated to more than 60^{o} while being connected to the vacuum line some of the surface adsorbed oxygen will remain. This amount of oxygen could bring about the oxidation of some of the porphyrins adsorbed on the surface. The Lewis-acid sites present on the surface of PVG can form weak charge transfer bonding. These sites may not be sufficiently strong acceptors for complete electron transfer as demonstrated by the experiments done in the absence of oxygen. Molecular oxygen complexes with these sites, and having done so, provide a path for complete electron transfer from the porphyrin. Another possibility is for the molecular oxygen to act as the direct electron acceptor. The electron can then be transferred to a Lewis acid site or to a Bronsted acid site.

(e) Decarbonylation Reactions

The difficulty experienced in carrying out the decarbonylation reaction catalytically can be attributed mainly to the stability of $Ru(TPP)(PBu^n_3)_2$ which is easily formed under the reaction conditions. This compound once formed does not substitute one of its PBu^n_3 ligands for CO from aldehyde under reaction conditions. Therefore the catalytic cycle is not continued. The correspodence to the authors indicated that they too had difficulty reproducing data.

(f) Conclusions

Only a few publications are available on studies of porphyrins adsorbed on solid supports. A recent publication[90] describes the resonance Raman spectra of porphyrins adsorbed on gamma-alumina and silica. As porphyrins have strong absorptions in the visible region they are being used as a pigment for initial harvest of energy from sunlight and subsequently transfer to such semiconductors as titanium oxide which do not absorb sunlight directly. Such uses will require the adsorption of porphyrins on solid surfaces. This study is an attempt to understand the nature of changes that these important chemical compounds undergo when adsorbed on a solid support.

5. BIBLIOGRAPHY

(1). Falk, J. E. "Porphyrins and metalloporphyrins", Elsevier, Amsterdam, 1964.

(2). Ann. N. Y. Acad. Sci. 1973, 206.

(3). "Porphyrins and metalloporphyrins", (Smith, K. M. ed.) Elsevier, Amsterdam, 1975.

(4). "The Porphyrins", Vol. I to VII, (Dolphin, D. ed.) Academic Press, New York, 1980.

(5). Buchler, J.W.: Puppe, L.: Rohbock, K.: Schneege, H. H. Ann. N. Y. Acad. Sci. 1973, 206, 116.

(6). Longuet-Higgins, H. C.: Rector, C. W. : Platt, J. R. J. Chem. Phys. 1950, 18, 1174.

(7). Gouterman, M. "The Porphyrins", (Dolphin D. ed.) Academic Press,New York,1979: Vol I, p 1.

(8). Becker, R. S. : Kasha, M. J. Am. Chem. Soc. 1975, 77, 3669.

(9). Hopf, F. R. and Whitten, D. G., "Porphyrins and Metalloporphyrins", (Smith, K. ed.) Elsevier, Amsterdam 1975.

(10). Becker, R. S. : Allison, J. B. J. Phys. Chem. 1963, 67, 2662.

(11). Eastwood, D. : Goutermann, M. J. Mol. Spectrosc. 1970, 35, 359.

(12). Lavalee, D. K. : Gebala, A. E. Inorg. Chem. 1973, 13, 2004.

(13). Hambright, P., "Porphyrins and Metalloporphyrins", (Smith, K. M. ed.) Elsevier, Amsterdam, 1975,p 238.

(14). Abraham, R. J.: Hawkes, G. E.: Hudson, M. F. : Smith, K. M. J. Chem. Soc. Perkin trans. 1975, 2, 204.

(15).Closs, G. L. : Closs, L. E. J. Am. Chem. Soc. 1963, 85, 818.

(16). Fuhrhop, J. H. : Mauzerall, D. J. Am. Chem. Soc. 1969, 91, 4147.

(17). Fuhrhop, J. H.: Kadish, K. M.: Davis, D. G. J. Am. Chem. Soc. 1973, 95, 5140.

(18). Felton, R. H., "The Porphyrins", (Dolphin, D. ed.), Academic Press, New York, 1979: Vol. V,p 53.

(19). Felton, R. H.: Dolphin, D.: Borg, D. C. : Fajer, J., J. Am. Chem. Soc. 1969, 91, 196.

(20). Dolphin, D.: Felton, R. H.: Borg, D. C. : Fajer, J., J. Am. Chem. Soc. 1970, 92, 743.

(21). Wolberg, A. : Manassen, J., J. Am. Chem. Soc. 1970, 92, 2983.

(22). Fajer, J.: Borg, D. C.: Forman, A.: Dolphin, D. : Felton, R. H., J. Am. Chem. Soc. 1970, 92, 3451.

(23). Fajer, J. : Davis, M. S., "The Porphyrins" (Dolphin, D. ed.), 1979: Vol. IV, p 197.

(24). Forman, A.: Borg, D. C.: Felton, R. H.: Fajer, J., J. Am. Chem. Soc. 1971, 93, 2790.

(25). Bard, A. J.: Ledwith, A. : Shine, H. J., Adv. in Phys. Org. Chem. 1976, 13, 155.

(26). Dolphin, D. : Felton, R. H., Acc. Chem. Res. 1974, 7, 26.

(27). Padilla, A. G.: Wu, S. M.: Shine, H. J. J. C. S. Chem. Comm. 1976, 236.

(28). Shine, H. J.: Padilla, A. G.: Wu, S. M. J. of Org. Chem. 1979, 101, 5953.

(29). Smith, K. M.: Barnett, G. H.: Evans, B. : Martynenko, Z., J. Am. Chem. Soc. 1979, 101, 5953.

(30). Guzinski, J. A. : Felton, R. H: J. Chem. Soc. Chem. Commun. 1973, 715.

(31). Gold, A.: Ivey, W. : Bowen, M: J. Chem. Soc. Chem. Commun. 1981, 293.

(32). Gold, A.: Ivey, W: Toney, G. E. : Sangiah, R: Inorg. Chem. 1984, 23, 2932.

(33). Dolphin, D.: Muljiani, Z.: Rousseau, K: Borg, D. C.: Fajer, J. : Felton R. H.: Ann. N. Y. Acad. Sci. U. S: 1971, 68, 614.

(34). Strekas, T. C. : Spiro, T. G.: Biochem. Biophys. Acta. 1972, 263, 830.

(35). Spiro, T. G. : Strekas, T. C.: Proc. Natl. Acad. Sci. 1972, 69, 2622.

(36). Felton, R. H. : Yu, N. T.: "The Porphyrins" (Dolphin, D. ed.), Academic press, New York, 1979: Vol. V, p.347 .

(37). Spiro, T. G.: "Iron Porphyrins" (Lever, A. B. P. : Gray, H. B. ed.), Addison-Wesley, 1983: Part 2, p.89 .

(38). Burke, J. M.: Kincaid, J. R. : Spiro, T. G: J. Am. Chem. Soc. 1978, 100, 6077.

(39). Fuchsman, W. H.: Smith, Q. R. : Stein, M. M.: J. Am. Chem. Soc. 1977, 99, 4190.

(40). Lutz, M. : Kleo, K.: Biochem. Biophys. Acta. 1979, 546, 365 .

(41). Cotten, T. M.: Parks, K. D. : Van Duyne, R. P.: J. Am. Chem. Soc. 1980, 102, 6399 .

(42). Yamaguchi, H.: Nakano, M. : Itoh, K.: Chem. Lett. 1982, 1397.

(43). Groves, J. T.: Nemo, T. E. : Myers, R. S.: J. Am.

Chem. Soc. 1979, 101, 1032 .

(44). Ulrich, V.: Top. Curr. Chem. 1979, 83, 68 .

(45). Dolphin, D. : James, B. R.: ACS Symp. Ser. 1983, 211, 99 .

(46). Groves, J. T. : Nemo, T. E.: J. Am. Chem. Soc. 1983, 105, 6243.

(47). Munsuy, D.: Bartoli, J. F: Chottard, J. C. : Lange, M: Angew. Chem. Int. Ed. Eng. 1980, 19, 909.

(48). Groves, J. T.: Kuper, W. J.: Nemo, T. E. : Meyers, R. S: J. Mol. Catal. 1980, 7, 169.

(49). Chang, C. K. : Kuo, M. S.: J. Am. Chem. Soc. 1979, 101, 3413.

(50). Shannon, P. : Bruice, T. C.: J. Am. Chem. Soc. 1981, 103, 4580.

(51). Hill, C. L. : Schardt, B. C.: J. Am. Chem. Soc. 1980, 102, 6374.

(52). Groves, J. T.: Kruper, W. J. : Haushalter, R. C.: J. Am. Chem. Soc. 1980, 102, 6375.

(53). Hill, C. L. : Smegal, J. A.: Nouv. J. Chim. 1982, 6, 287.

(54). Tabushi, I. : Koga, N.: Tetrahedron Lett. 1979, 3681.

(55). Tabushi, I. : Yazaki, A.: J. Am. Chem. Soc. 1981, 103, 7371.

(56). Groves, J. T. : Kruper, W. J.: J. Am. Chem. Soc. 1979, 101, 7613..

(57). Hickman, D. L. : Goff, H. M.: Inorg. Chem. 1983, 22, 2787.

(58). Parmon, V. N.: Lymar, S. V: Tsvetkov, I. M. : Zamaraev, K. I: J. Mol. Catal. 1983, 21, 353.

(59). Kobayashi, N. : Osa, T.: J. Electroanal. Chem. 1983, 157, 269.

(60). Buttry, D. A. : Anson, F. C.: J. Am. Chem. Soc. 1984, 106, 59.

(61). Pawlik, M.: Hoq, M. F.: Shepherd, R. E.: J. Chem. Soc. Chem. commun. 1983, 1467.

(62). Mochida, I.: Yasutake, A.: Fujitsu, H. : Takeshita, K.: J. Phys. Chem. 1982, 86, 3468.

(63). Lever, A. B. P.: Ramaswamy, B. S. : Licoccia, S.: J. Photochem. 1982, 19, 173.

(64). Durand, R. R. Jr.: Bencosme, C.: Collman, J. P. : Anson, F. C.: J. Am. Chem. Soc. 1983, 105, 2710.

(65). Domazetis, G.: Tarpey, B.: Dolphin, D. : James, B. R.: J. Chem. Soc. Chem. Commun. 1980, 939.

(66). Domazetis, G.: James, B. R.: Tarpey, B. : Dolphin, D.: ACS Symp. Ser. 1981, 152.

(67). Iler, K.: "The Chemistry of Silica", Wiley-Interscience, New York, 1979: p 572.

(68). Elmer, T. H. : Nordberg, M. E.: "Materials in Design Engineering", Reinhold Publishing Corporation, New York, december 1962.

(69). Yamada, H. : Yamamoto, Y.: J. Chem. Soc. Faraday Trans I. 1979, 75, 1215.

(70). Simon, R.: Gafney, H. D. : Morse, D. L.: Inorg. Chem. 1983, 22, 573.

(71). Low, M. J. D. : Subra Rao, V. V.: Canad. J. Chem. 1968, 46, 3255.

(72). Egerton, T. A.: Hardin, A. H.: Kozirovski, Y. : Sheppard, N.: Chem. Comm. 1971, 887.

(73). Buechler, E. : Turkevich, J.: J. Phys. Chem. 1972, 76, 2325.

(74). Turkevich, J. : Fujita, Y.: Science 1966, 152, 1619.

(75). Dollish, x. : Hall, X.: J. Phys. Chem. 1965, 69, 4402.

(76). Yamamoto, Y. : Yamada, H.: J. Chem. Soc. Faraday Trans I. 1978, 74, 1562.

(77). Yamada, H.: Appl. Spectrosc. Rev. 1981, 17, 227.

(78). Yamamoto, Y.: Yamada, H.: J. Raman Spectrosc. 1982, 12, 157.

(79). Stamires, S. : Turkevich, J.: J. Am. Chem. Soc. 1964, 86, 749.

(80). Chow, B. : Cohen, I. A.: Bioinorg. Chem. 1971, 1, 57.

(81). Tsutsui, M.: Ostfeld, D. : Frances, J. N: J. Coord. Chem. 1971, 1, 115.

(82). Rillema, D. P.: Nagle, J. K.: Barringer, L. F. : Meyer, T. J.: J. Am. Chem. Soc. 1981, 103, 56.

(83). Adler, A.: Longo, F. R.: Kampas, F. : Kim, J.: J. Inorg. Nucl. Chem. 1970, 32, 2443.

(84). Kenelly, T. : Gafney, H.D.: J. Inorg. Nucl. Chem. 1981, 43, 2988.

(85). Basu, A.: Gafney, H. D.: Perettie, D. J. : Clark, J. B.: J. Phys. Chem. 1983, 87, 4532.

(86). Valence, W. G. : Strekas, T. C.: J. Phys. Chem. 1982, 86, 1804.

(87). Meites, L.: Ed: H:book of Analytical Chemistry, pp.5-12 and 11-5 to 11-7, McGraw Hill, Inc: New York 1963.

(88). Boschi, T.: Bontempelli, G. : Mazzocchin, G.: Inorg. Chim. Acta, 1979, 37, 155.

(89). Stone, A. : Fleischer, E. B.: J. Am. Chem. Soc. 1968,

90, 2735.

(90). Streusand, B. J. : Schrader, G. L.: Appl. Spectrosc. 1984, 38, 433.

(92). Phillips, J. N.: Rev. Pure and Appl. Chem: 1960, 10, 35.

(92). Knowles, P. F.: Marsh, D. : Rattle, H. W. E.: "Magnetic Resonance of Biomolecules" John Wiley & Sons, New York, 1976: p 181.